THE ANGULAR CORRELATION OF ANNIHILATION RADIATION AND A STUDY OF HIGH ENERGY NUCLEAR REACTIONS IN NEON.

by

KARL LEMBIT ERDMAN

A THESIS SUBMITTED IN PARTIAL FULFILMENT OF
THE REQUIREMENTS FOR THE DEGREE OF
DOCTOR OF PHILOSOPHY
IN PHYSICS

We accept this thesis as conforming to the standard required from candidates for the degree of DOCTOR OF PHILOSOPHY IN PHYSICS

Members of the Department of Physics

THE UNIVERSITY OF BRITISH COLUMBIA

May, 1953.

ABSTRACT

In the first section of this thesis the measurement of the angular correlation of annihilation radiation in various materials is described. It is found that the angular dependence of the coincidence counting rate leads to results which are not in agreement with the present theories of the mechanism of positron decay processesin crystal and metal lattices. In particular, positrons do not appear always to reach thermal energies before annihilation with electrons takes place.

A search for the photodisintegration of Ne^{20} using the gamma rays from the $Li^7(p,\gamma)Be^8$ reaction is described. An unusually low cross-section for the photo-alpha process to the ground state of O^{16} is found, 8×10^{-30} cm^2 for the 17.6 Mev. gamma ray and 3×10^{-29} cm^2 for the 14.8 Mev. gamma ray. Cross-sections of the order of 10^{-28} cm^2 are obtained for alpha particle transitions to the 6 and 7 Mev. excited state of O^{16}. These cross-sections are of the usual order of magnitude for photodisintegration reactions.

Irradiation of Ne^{20} with high energy neutrons gives rise to alpha particle transitions from the Ne^{21} compound nuclear levels so formed to several excited states of O^{17}. The excitation energies of these states are in good agreement with those measured in other nuclear reactions.

THE UNIVERSITY OF BRITISH COLUMBIA
Faculty of Graduate Studies

PROGRAMME OF THE FINAL ORAL EXAMINATION FOR THE DEGREE OF DOCTOR OF PHILOSOPHY

of

KARL LEMBIT ERDMAN

B.Sc. (University of Alberta) 1948
M.Sc. (University of Alberta) 1949

FRIDAY, MAY 8th, 1953, at 10:00 A.M.
IN ROOM 300 PHYSICS BUILDING

COMMITTEE IN CHARGE:

H. F. Angus, *Chairman*

C. A. Barnes	W. A. Bryce
K. C. Mann	H. C. Gunning
G. M. Shrum	S. A. Jennings
J. B. Warren	B. Savery

LIST OF PUBLICATIONS

Positive Particles Associated with Beta-ray Emitters, K. L. Erdman, G. Kokotailo, D.B. Scott, Physical Review 76, 1262, 1949.

THESIS

THE ANGULAR CORRELATION OF ANNIHILATION RADIATION AND A STUDY OF HIGH ENERGY NUCLEAR REACTIONS IN NEON

In the first section of this thesis the measurement of the angular correlation of annihilation radiation in various materials is described. It is found that the angular dependence of the coincidence counting rate leads to results which are not in agreement with the present theories of the mechanism of positron decay process in crystal and metal lattices. In particular, positrons do not appear always to reach thermal energies before annihilation with electrons takes place.

A search for the photodisintegration of Ne^{20} using the gamma rays from the $Li^7(p,\gamma)Be^8$ reaction is described. An unusually low cross-section for the photo-alpha process to the ground state of O^{16} is found, 8×10^{-30} cm^2 for the 17.6 Mev. gamma ray and 3×10^{-29} cm^2 for the 14.8 Mev. gamma ray. Cross-sections of the order of 10^{-28} cm^2, are obtained for alpha particle transitions to the 6 and 7 Mev. excited states of O^{16}. These cross-sections are of the usual order of magnitude for photodisintegration reactions.

Irradiation of Ne^{20} with high energy neutrons gives rise to alpha particle transitions from the Ne^{21} compound nuclear levels so formed to several excited states of O^{17}. The excitation energies of these states are in good agreement with those measured in other nuclear reactions.

GRADUATE STUDIES

Field of Study: Physics

Spectroscopy -- K. B. Newbound
Electromagnetic Theory -- W. Opechowski
Nuclear Physics -- K. C. Mann
Quantum Mechanics -- G. M. Volkoff
Chemical Physics -- A. J. Dekker
Radiation Theory -- F. A. Kaempffer
Theoretical Nuclear Physics -- G. M. Volkoff

Other Studies:

Probability and Statistics -- E. S. Keeping
Advanced Differential Equations -- T. E. Hull
Radiochemistry -- M. Kirsch and K. Starke

TABLE OF CONTENTS

PART II - THE PHOTODISINTEGRATION OF NEON

PART III - DISINTEGRATION OF NEON BY FAST NEUTRONS

TABLE OF ILLUSTRATIONS

ACKNOWLEDGEMENTS

The author is indebted to Dr. J. B. Warren for his kind supervision of the work which was done in this thesis and, in particular, for the experiment on positron annihilation which was first suggested by him.

The experiment on the angular correlation of annihilation quanta was made possible by the opportunity of working at the Chalk River pile and the suggestions and help given by Dr. L. G. Elliott and Mr. E. P. Hincks.

It is a pleasure to acknowledge the aid and suggestions of the many members and staff of the Physics Department in the experiments conducted with neon. In particular, thanks are given to Dr. C. A. Barnes for his discussions on the photo-disintegration of the neon nucleus and to Dr. D. B. James for his valuable aid in making the measurements.

The author's part in this work was made possible by scholarships awarded by the National Research Council and by the British Columbia Telephone Company.

PART I

THE ANGULAR CORRELATION OF ANNIHILATION RADIATION

I. INTRODUCTION

The radiation from the annihilation of positron electron pairs was first shown to be made up of pairs of coincident quanta emitted in opposite directions by Klemperer[46]. Calculations based on the Dirac hole theory[1] show that all but a few percent of the positrons reach the end of their path of ionization before annihilating. If the energy of the positron is small, a relationship can be developed between the momentum of the annihilating pair and the angle between the two annihilation quanta. By

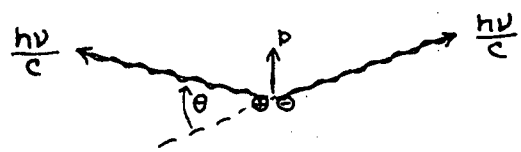

the laws of the conservation of energy and momentum it can be seen that:

$$2h\nu = mc^2 \left(1 + \frac{1}{\sqrt{1 - B^2}}\right)$$

and

$$p = \frac{2h\nu}{c} \sin \theta/2$$

where

$$B = v/c$$

by eliminating $h\nu$ we have $p = mc\left(1 + \frac{1}{\sqrt{1 - B^2}}\right) \sin \theta/2$.

If the momentum is small then v is small and by neglecting B^2, $p/mc \approx 2 \sin \theta/2$, and since θ will also be small then

$$\frac{p}{mc} \approx \theta$$

An attempt to measure the coincidence rate as a function of this angle was made by Beringer and Montgomery[47] using Geiger counters as detectors. The negative result together with the increased detection efficiency of scintillation crystals and photomultipliers led to a further investigation by Argyle and Warren[3] and De Benedetti, Cowan, Konneker and Primakoff[2]. Calculations made by De Benedetti and his co-workers seemed to indicate that the slowed-down positrons lost their remaining kinetic energy by collisions with the crystal lattice in a time of the order of 3×10^{-10} seconds, and the thermalized positrons proceeded to wander about in spaces of the crystal or metal lattice not precluded by the positive ions until they found a suitable mating electron, taking a time of the order of 10^{-9} seconds. The momentum distribution of the annihilating pairs could therefore be expected to be the momentum distribution of the combining electrons in the lattice, so in the case of a metal these would be expected to be the conduction electrons.

The observed exponential dependence of the coincidence rate with the angle θ in copper, of the form $Nc = No\, e^{-k\theta/\theta_o}$, gave an average momentum for the electrons in copper which was close to the theoretically predicted average momentum for the conduction electrons. It was noted by Warren and Griffiths[4] that all of the

measurements did not give a simple exponential result, and furthermore that the average momentum, although reasonable, did not vary in a too systematic way among the materials tested. A further measurement of this last effect was carried out by H. Maier Leibnitz[5] who noticed that in some cases the change in momenta was entirely in the wrong direction from what would be expected on the basis of electronic shell structure.

To gain more information about the way in which the average momentum varied among various substances, it was felt that measurements should be made with increased angular resolution, geometry which involved few corrections, and with the angular range extended as far as possible.

II. EXPERIMENTAL ARRANGEMENT

(a) Source

The source of positrons was a .0005" foil of copper of size 1 cm. x 3 cm. The thickness was chosen so that 90 percent of the positrons escaped from the foil before annihilation. This was done by assuming the momentum distribution was that predicted by the beta decay theory of Fermi with an end point corresponding to 0.66 Mev. Calculations by Heitler[1], mentioned earlier, on the small amount of high energy annihilation also allowed the assumption that the Feather range energy relationship for beta particles would apply for positrons, in which case the maximum range of the fastest positron should be equal to the thickness of absorber corresponding to a mass of 0.24 gms. per cm^2.

The electrolytically pure copper was irradiated in a flux of 2×10^{13} neutrons/sec. in the N.R.X. pile at Chalk River for periods of about 24 hours. At this time the activity due to annihilation radiation corresponded to 300 millicuries. The foils were placed between two sheets of absorber of thickness corresponding to the maximum range of the positrons and the assembly was placed in a slot in a 1" round rod of styrofoam (air-filled polystyrene

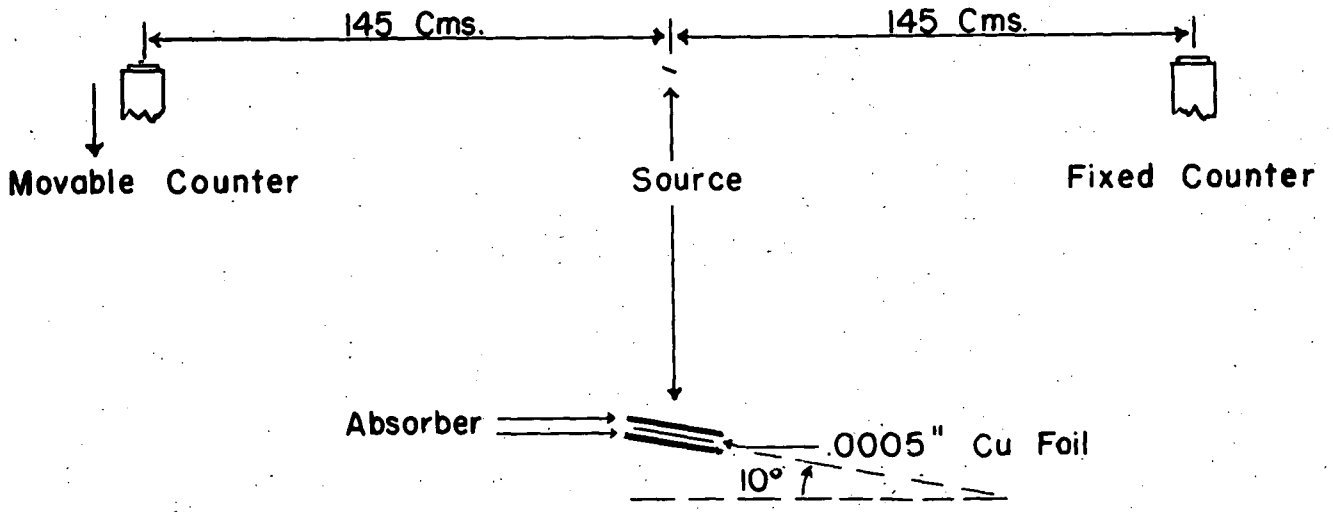

Fig. I Experimental Arrangement

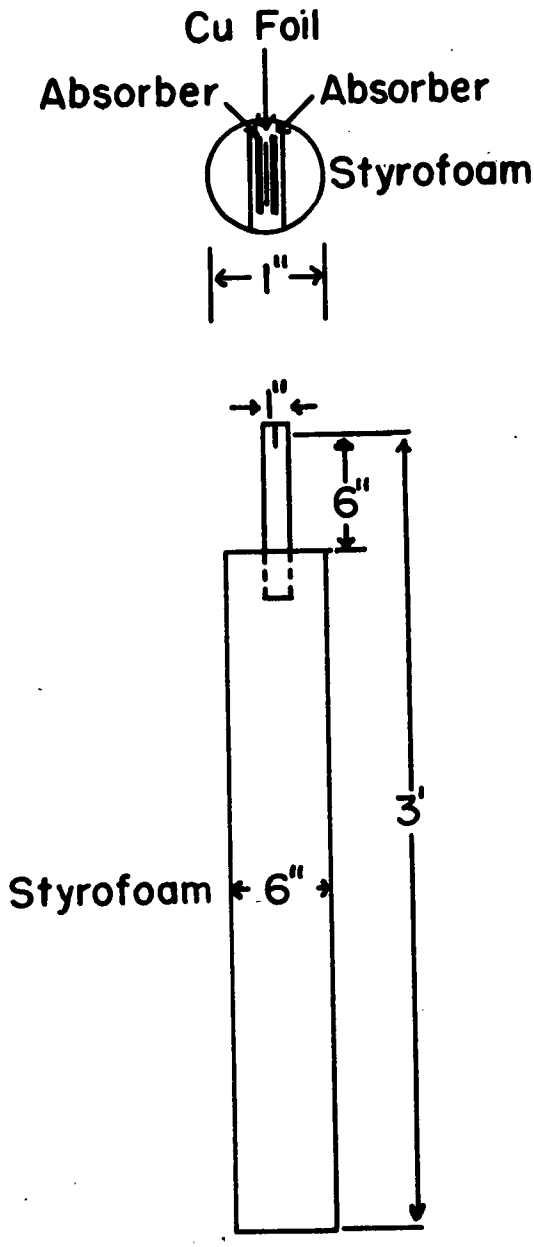

Fig. II Source Mount

of density 0.02 gm./cm.^{3}) which was fastened to a larger block of the same material for rigidity (Figure II). The source was placed midway between two detectors at a height of 3' above the floor.

(b) Detectors and Geometry

The gamma-ray detectors consisted of two E.M.I. photo-multipliers, run at 2800 volts supplied from Chalk River Mk VIIa H.T. units, with 1" x $1\frac{1}{4}$" x $\frac{1}{4}$" slices of trans-stilbene mounted on the photocathodes. Trans-stilbene was used due to its high speed as a phosphor. The detection efficiency per gamma quantum of .51 Mev. radiation is 0.27 per inch of crystal thickness. Dow Corning DC 200 silicone oil of 20,000 centistokes viscosity was used as the light coupling medium between the crystals and the multipliers. The crystals were covered with 0.001" aluminum foil and the assembly was made light tight by wrapping with black Scotch brand cellulose electrician's tape.

The counters were positioned 290 cm. apart with the source midway between them (Figure I). One counter was rigidly fastened to the end of a table; the other was fastened to the carriage of a travelling microscope. The vernier scale of this instrument thus acted as the azimuthal angle indicator.

The 180° counter-source-counter line was established roughly with a tightly stretched thread fastened to the face of the fixed counter, passing through the source and over the face of the movable counter. The central line was established more exactly in each individual run by counting over this position.

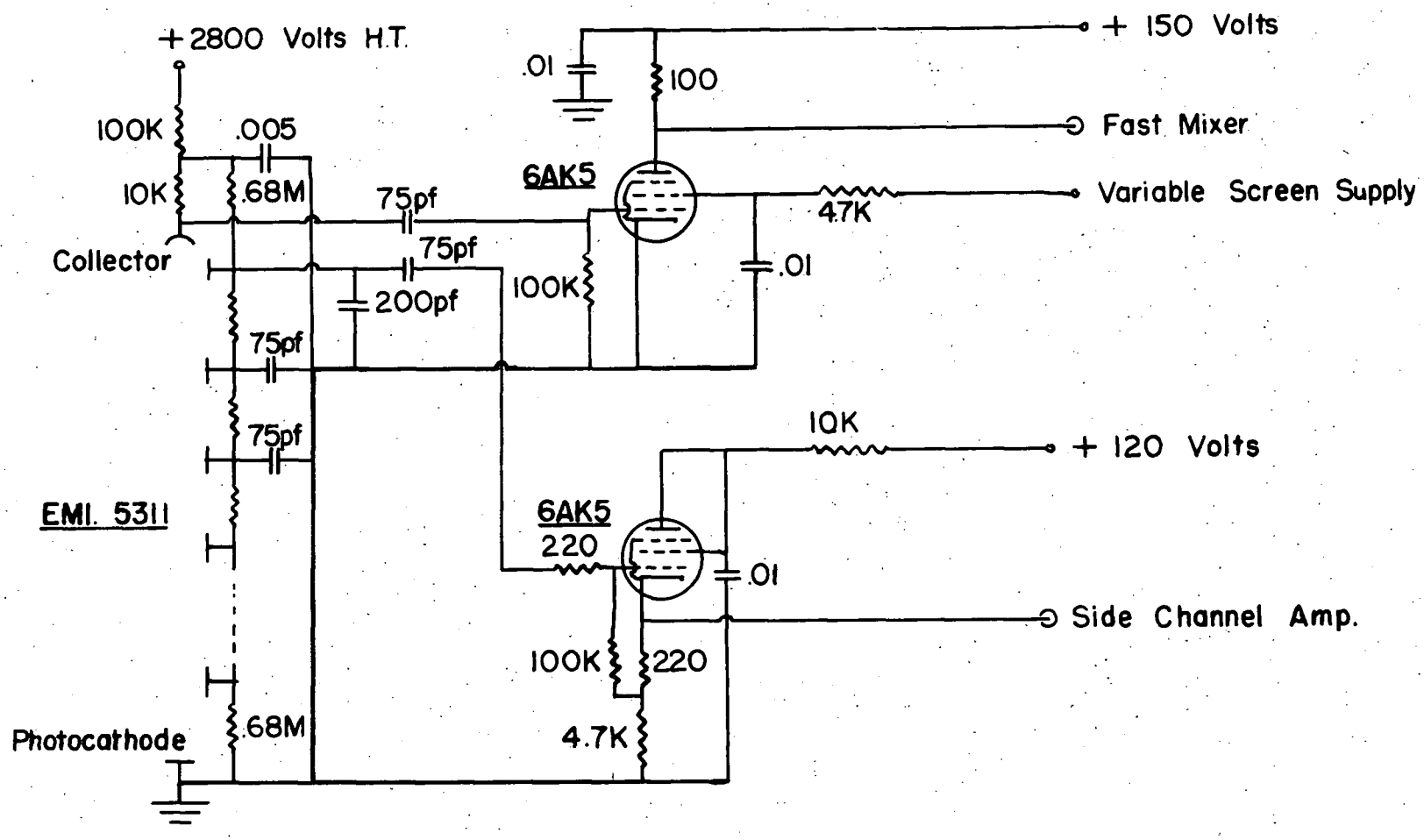

Fig. III Photomultiplier Circuit

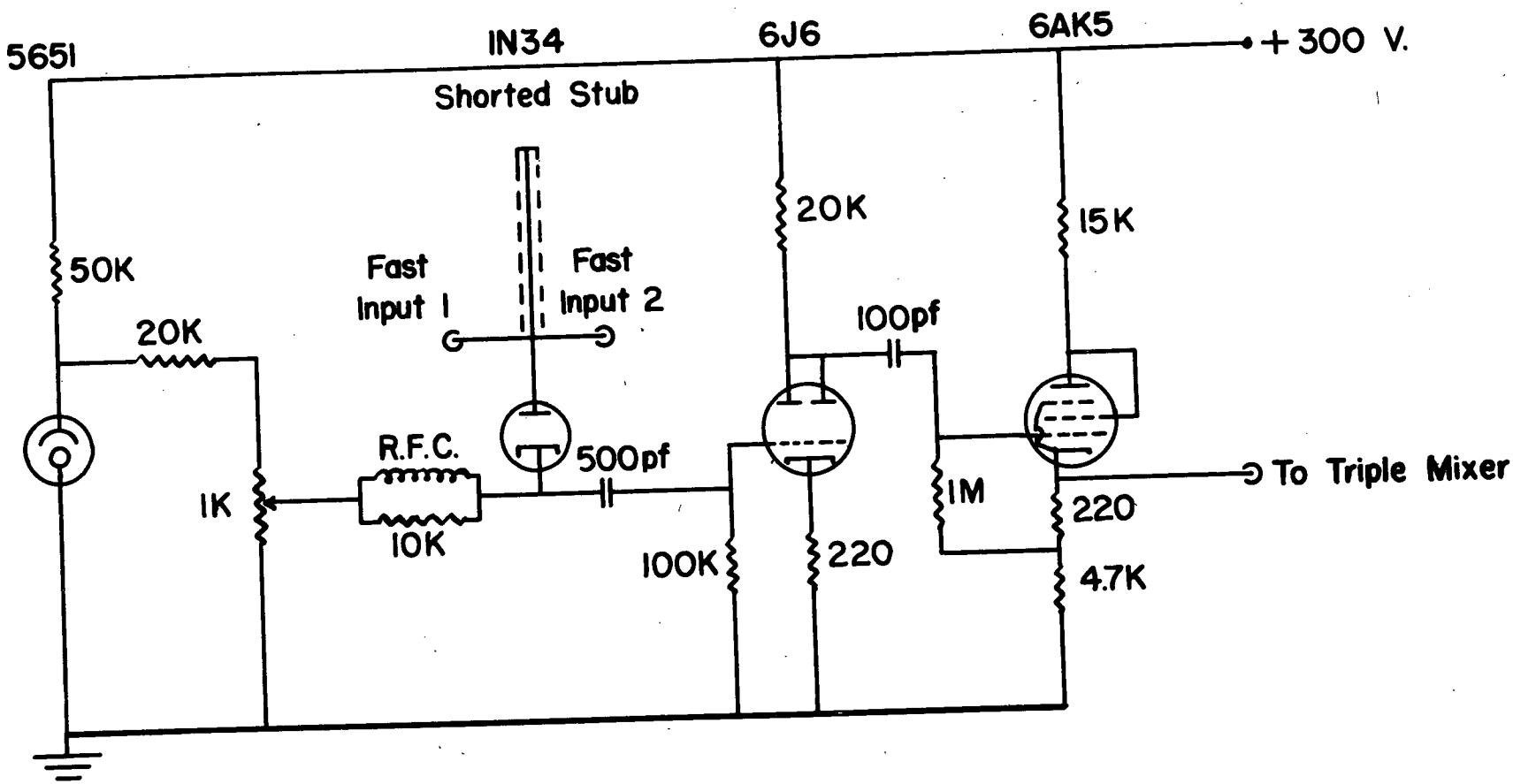

Fig. IV Fast Coincidence Mixer

As shown in Figure I the source was turned through a small angle. This served two purposes:

(i) The gamma-ray absorption path through the source was decreased.

(ii) The "width" of the source contributing to the geometrical overlap of the counters and the source was constant for absorbers of varying density since it now was a function of the width of the foil and the angle of the source and to a lesser extent of the thickness of the absorber used.

The source subtended an angle of 0.08° in the horizontal plane at the detector. The detectors subtended angles of 0.25° in this plane at the source. With this geometry, the counting rates obtained per detector were of the order of 80,000 counts per minute for a 200 millicurie positron source.

(c) Coincidence Counting Circuits

The pulses from the photomultipliers were fed into a coincidence circuit of the Bell-Petch type[6]. Pulses were taken from both the collector and final dynode of the photomultipliers (Figure III). A $\frac{1}{4}$ volt rise on the collector was sufficient to cut off the 6 AK5 pulse shaper. The standing current in this tube was controlled by the screen voltage. The shaped pulses travelled down 100 ohm co-axial lines to a 50 ohm shorted stub and diode (Figure IV). The level of the diode was set by varying the bias with counts in one channel only. Pulses from this point were passed to an Atomic Instruments amplifier (Model 204-C) with a rise time of 0.1 microseconds and a gain of 1000. The discriminated output was fed to a triple coincidence mixer with a resolving time of 1 microsecond.

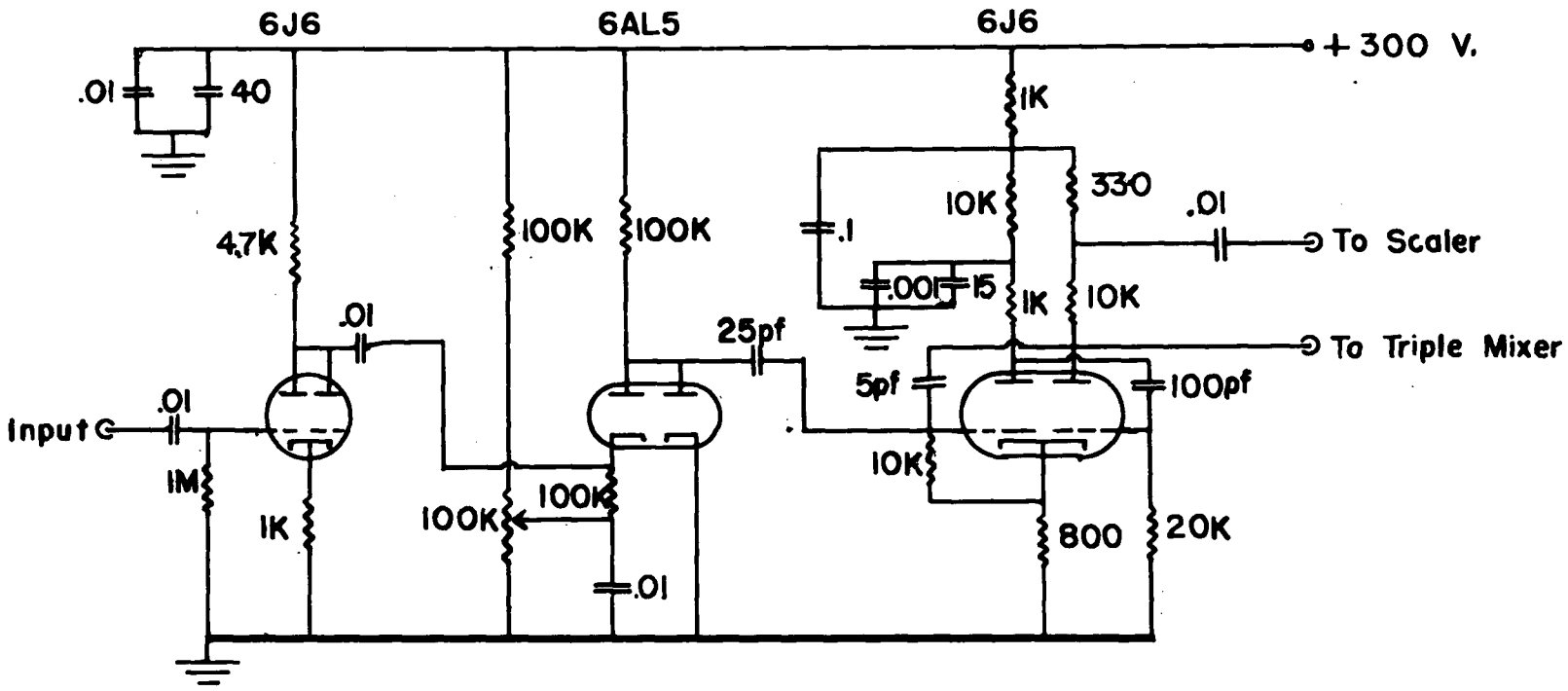

Fig. V Side Channel Amplifier and Discriminator

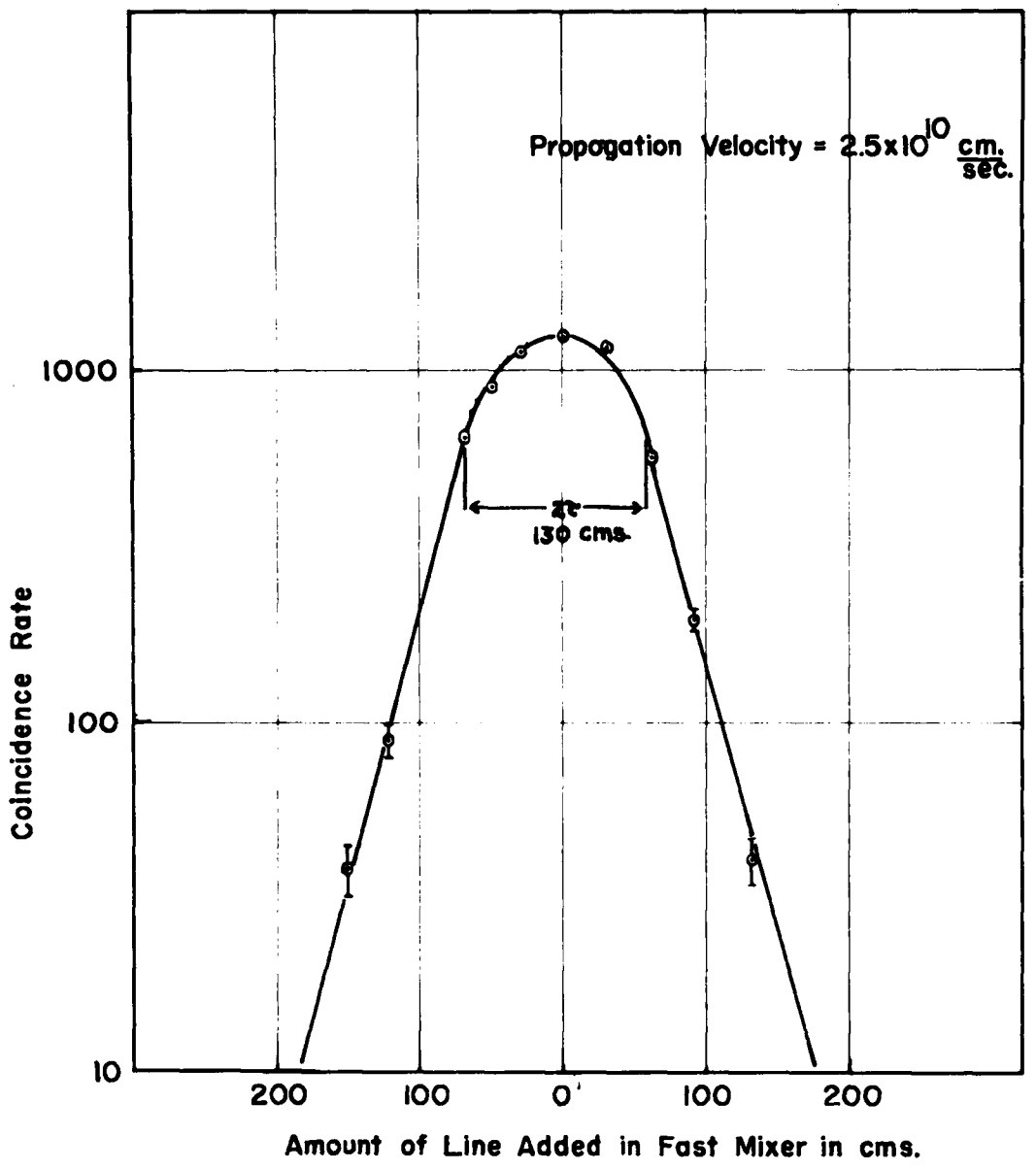

Fig. VI Measurement of Resolving Time by Pulse Delay Method

The side channel amplifiers (Figure V) were driven by the cathode followers on the final dynodes. Discrimination was carried out at a level high enough to remove a large fraction of the noise pulses and the discriminated output was monitored and fed to the triple coincidence mixer. Coincidences occuring in the mixer represented the desired coincidence count.

Monitoring was carried out with N.R.C. scales of 128.

(d) Measurement of Resolving Time

The resolving time of the circuit was measured in two ways.

(i) The counters were placed closely together and a source of positrons was placed between them. The length of 100 ohm (RG7U) cable between one pulse shaper and the fast coincidence mixer was then varied. This gave a curve of coincidence rate as plotted against length of delay cable used. By the use of the velocity of propogation of a wave in a cable of this type the time delay in the pulses was known and the resolving time could be read directly from the curve (Figure VI).

(ii) A random coincidence rate was taken with the counters at a large angle from co-linearity. The resolving time was calculated from the known single channel rates and the equation

$$T = \frac{N \text{ random}}{2N_1N_2} .$$

The resolving time measured by both of these methods was the same and was equal to $2.0 \pm .1 \times 10^{-9}$ sec.

When a fast phosphor such as trans-stilbene is used, the resolving time of a circuit of the above type is largely determined by the statistical variations in the time required for the

the first electron from the photocathode to reach the first dynode of the photomultiplier. Due to the long drift space in the 5311 E.M.I. photomultiplier, it is difficult to achieve resolving times as short as can be attained by the use of a tube with a short photocathode to dynode distance such as the 1P21.

(e) Experimental Procedure

Sources obtained from the pile were immediately mounted as previously described. The central position or position at 180° geometry of the annihilation gamma rays was established by counting over the central region.

A short check on the resolving time was made by placing the counters in the 180° position and varying the cable length of one counter and comparing the curve of counting rate versus pulse delay with the curve used for obtaining the resolving time.

The coincidence rate v.s. angle curve was taken beginning at large values of θ and ending at the position of co-linearity.

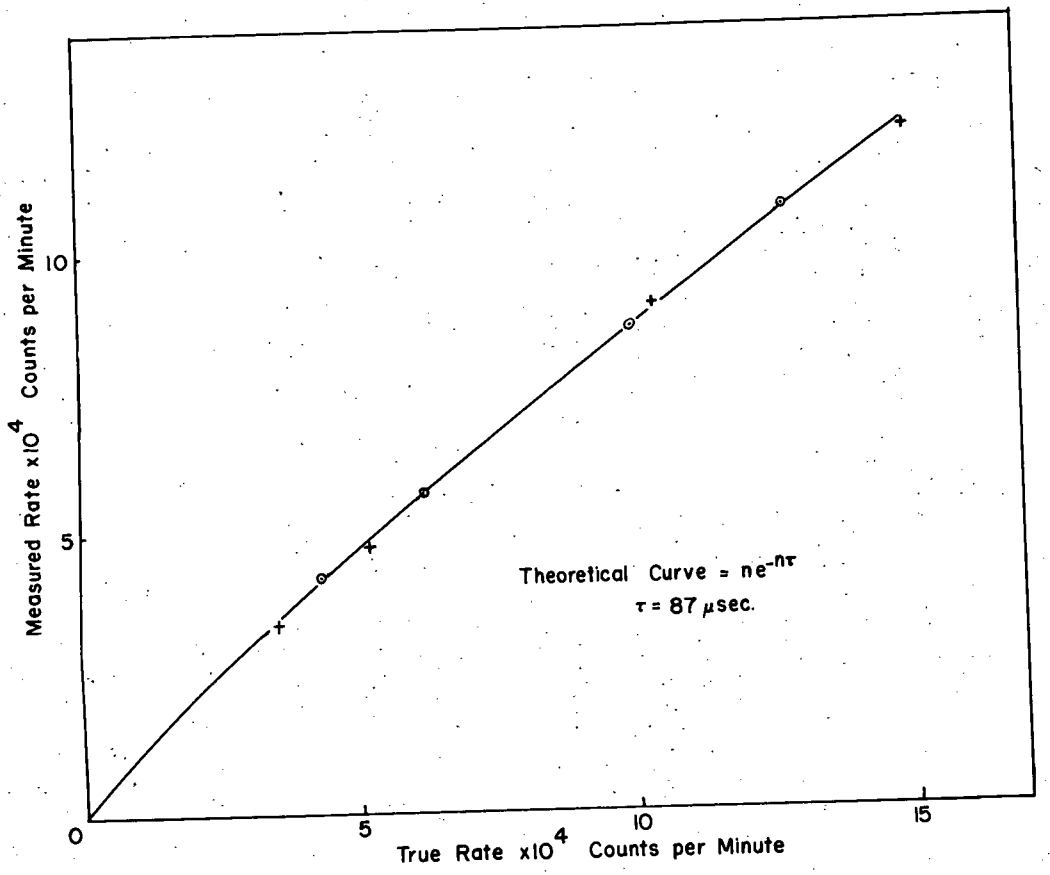

Fig. VII Dead Time of Circuits

III. CORRECTIONS TO OBSERVED DATA

(a) Counting Corrections

The observed coincidence rate was first corrected for dead times in the circuitry. This dead time correction was absolutely determined by the use of several of the 0.0005" copper foils, having a low activity, with an absorber of copper to stop all of the positrons. The counting rate for each foil alone in the absorber was measured. The counting rate for several foils was taken and plotted against the counting rate from the addition of the rates of single foils (Figure VII). Since the dead time losses for the single foils were negligible due to the low counting rates, the 87 microsecond dead time of the circuit may be considered to be a good approximation of the true dead time.

The decay correction for a half life of 12.88 hours[7] was applied to the counting rates.

(b) Geometrical Corrections

As is pointed out by Griffiths and Warren[4] a finite source and counter width has an effect of decreasing the slope of the log coincidence rate v.s. angle curve, if this curve is a pure exponential. Since the experiment was carried out to determine

a dependence of this curve on some property of the absorber and no absolute measurement was to be made, no correction for the finite widths and lengths of the source and counters was applied. As was outlined before, by suitable arrangement these were kept the same for all the absorbers.

(c) Scattering Corrections

(i) Compton Scattering The "good" geometry of the experiment reduces the Compton scattered quantum counting rate to a negligible value. Since the solid angle subtended at the source by the counter is only $4\pi \times 10^{-4}$ steradians and since the Compton cross section for this energy is not far from isotropic it is easy to see that the counter would only receive $\frac{1}{10^4}$ part of the total scattered radiation. Since the source was positioned as far as possible from any significant mass of surrounding material, there is likewise little effect from external scattering.

(ii) Rayleigh Scattering Coherent scattering of gamma ray by atoms has been demonstrated by Moon[8] to be up to 100 times as great as Compton scattering at small angles. Measurements made by Storruste[9] have agreed with the cross section values as calculated by Franz[10] for this process. The differential cross section for Rayliegh scattering may be written $d\sigma = \frac{e^4 A^2}{(m_o c)^2}$ where A^2 is obtained from the x-ray scattering considerations of Debye[11] (See Appendix I) who has given $\frac{A^2 u}{Z^2}$ as a function of u.

$$u = 2.43 \times 10^2 Z^{-1/3} \frac{E}{m_o c^2} \sin \theta/2$$

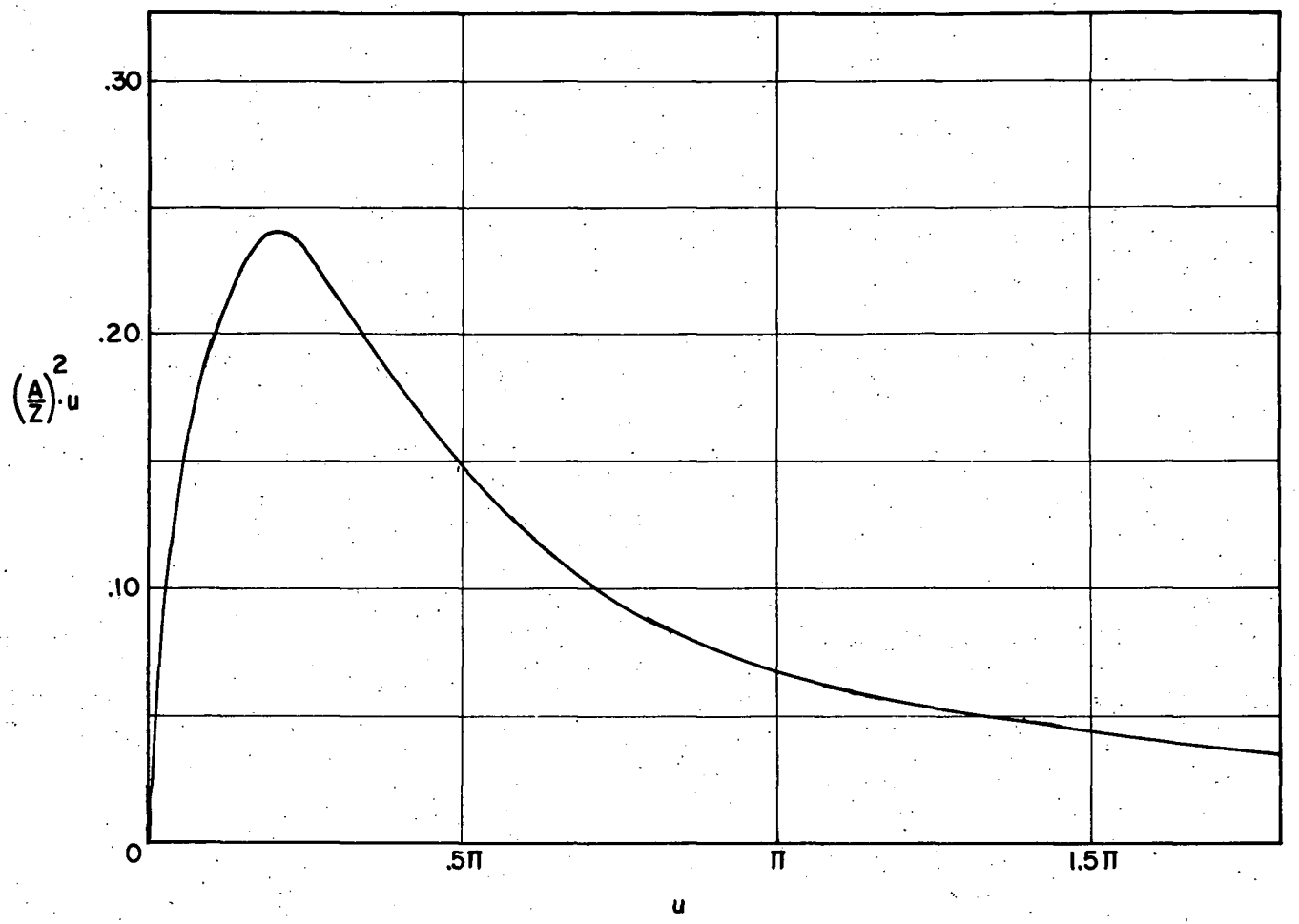

Fig. VIII Scattering Amplitude as a Function of Angle from P. Debye, Zeits. fur Phys. 1935

A = differential scattering amplitude at angle θ

E = energy of the quanta being scattered

θ = angle of scattering

$m_o c^2$ = rest energy of the electron

Z = atomic number of the scatterer.

The curve of Debye was extended to large and small values of u (Figure VIII). Using these results an absolute correction for single Rayleigh scattering was made to the experimental data. The magnitude of this correction is shown in (Figure IX) where the dashed curve represents a plot of the uncorrected coincidence rate. The large Z dependence which can be seen by the absence of an appreciable correction for Lithium is more obvious if one considers the region where $\frac{A^2 u}{Z^2}$ is almost a constant. Here Moon[8] has written the cross section as

$$S_R = \frac{8.67 \times 10^{-33}}{\sin^3 \theta/2} \left(\frac{Z m_o c^2}{E}\right)^3 \times \frac{(1 + \cos^2 \theta)}{2} \text{ cm.}^2.$$

The Rayleigh cross section for various angles was calculated from Franz's equations. (A private communication from Professor P.B. Moon confirmed that their measurements agreed with the absolute magnitude of the number of scattered quanta as calculated from the formulae.) The assumption was made that in any one annihilation only one scattering event occurred. The thickness of scatterer was therefore taken as the thickness of source crossed by a line between the counters when they were in the position of

colinearity. Since the experimental Nc v.s. θ curve drops so rapidly with angle it is easy to see that only the scattering from the central region to the sides will have a significant effect on the counting rate. A numerical integration was carried out over the experimentally obtained Nc v.s. θ curve using the calculated cross section for scattering into the solid angle subtended by the counter at various angles. The curve so obtained for scattered quanta was then subtracted from the experimental curve. Thus for gold the cross section for scattering into the detector varied from 4×10^{-26} cm.^{2} at 0.4° to 1×10^{-26} cm.^{2} at 2.0°. The large Z dependence reduced these values by a factor of 1000 in the case of Li. The largest correction was obtained for Uranium and was 0.8 counts per minute at an angle of 1.2° when the coincidence peak height was 1600 counts per minute.

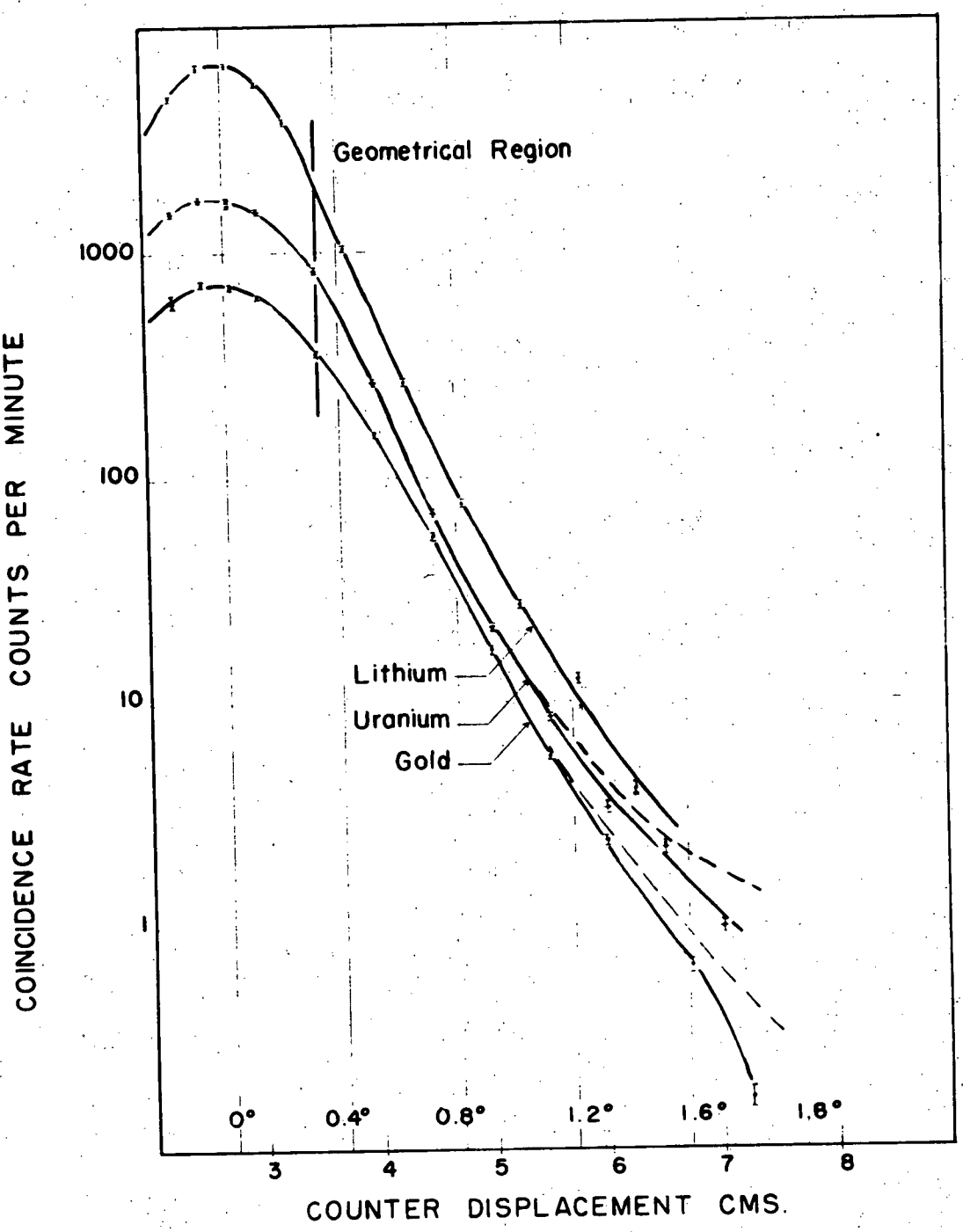

Fig. IX Effect of Correction for Rayleigh Scattering

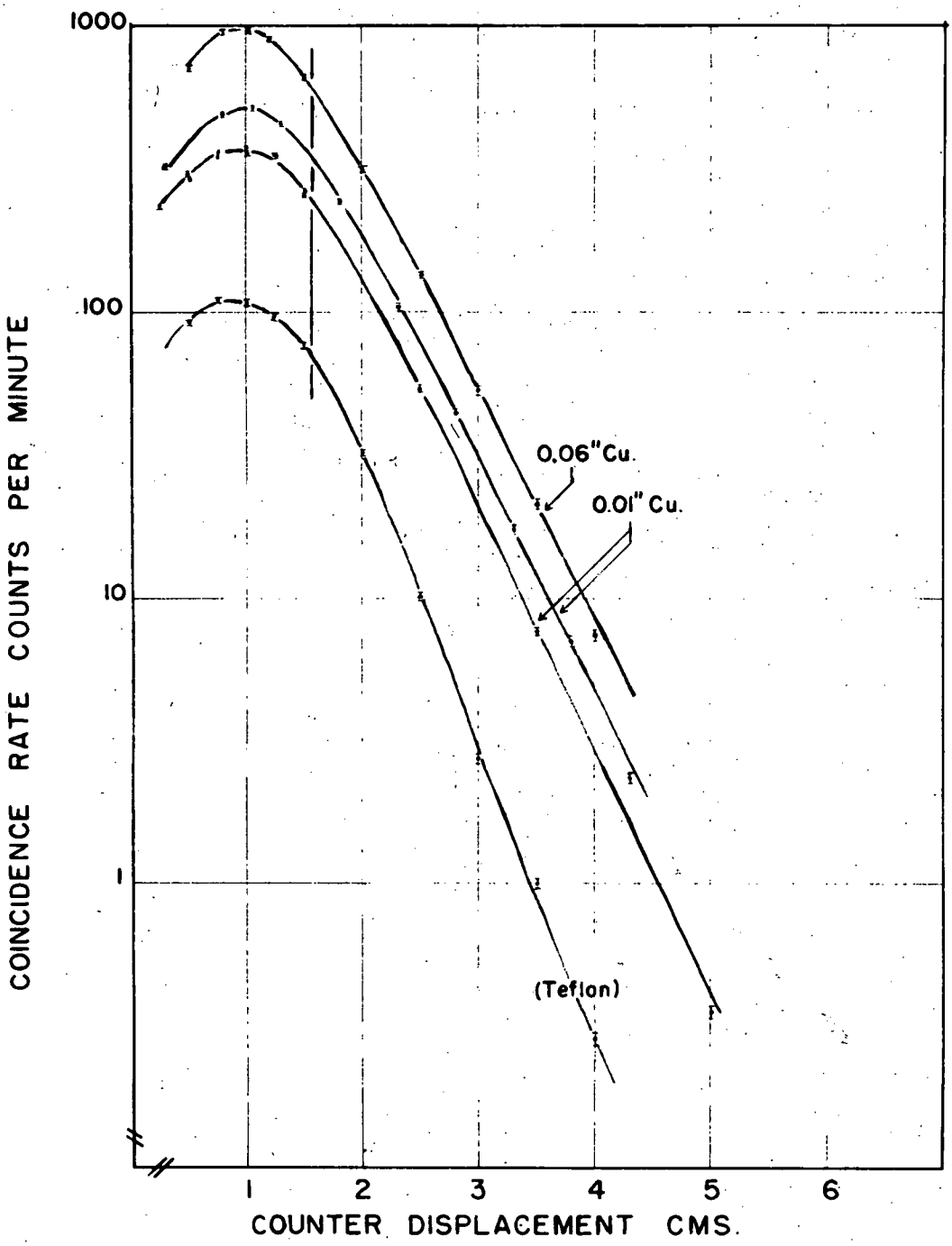

Fig. X Angular Correlation for Annihilation in Copper and Teflon

IV. RESULTS

(a) Annihilation in Copper

A comparison of the results obtained (Figure X) with those of previous workers shows good agreement. θ_o uncorrected for finite source and counter width (3.80×10^{-3} radians) agrees with the value given by Griffiths and Warren[4] (3.81×10^{-3} radians). The thickness of absorber was increased by a factor of 6 to determine the effect of scattering and was found to make no significant difference to the shape or the slope of the logarithmic plot.

An exponential type of dependence of the form $N_c = N_o e^{-k\theta/\theta_o}$ where N_o and θ_o are constants fits well, in which case the average value for the momentum calculated from $p_{av.} = 2\ mc\theta_o$ is 7.2×10^{-3} mc and $E_{av.} = 22$ ev.

Of the remaining absorbers only teflon gave a dependence of this simple exponential type so it is displayed in the same figure. θ_o for teflon was different from that of copper, giving an average p of 5.8×10^{-3} mc. and an $E_{av.} = 13$ ev.

(b) Other Substances

A series of 18 metals, salts and co-valent compounds were used as absorbers in an attempt to establish a dependence of the

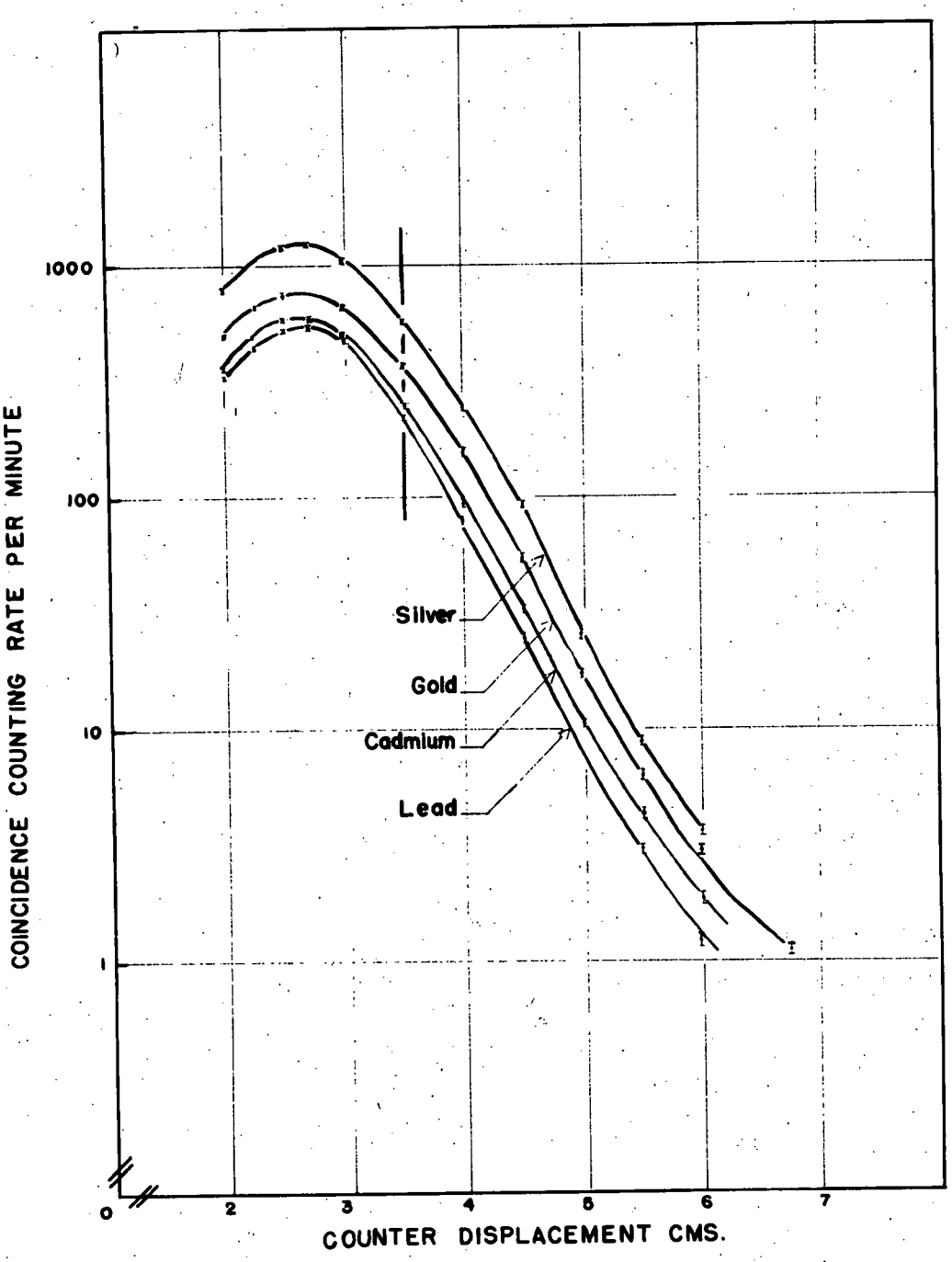

Fig. XI Angular Correlation for Annihilation in Ag, Au, Cd, Pb

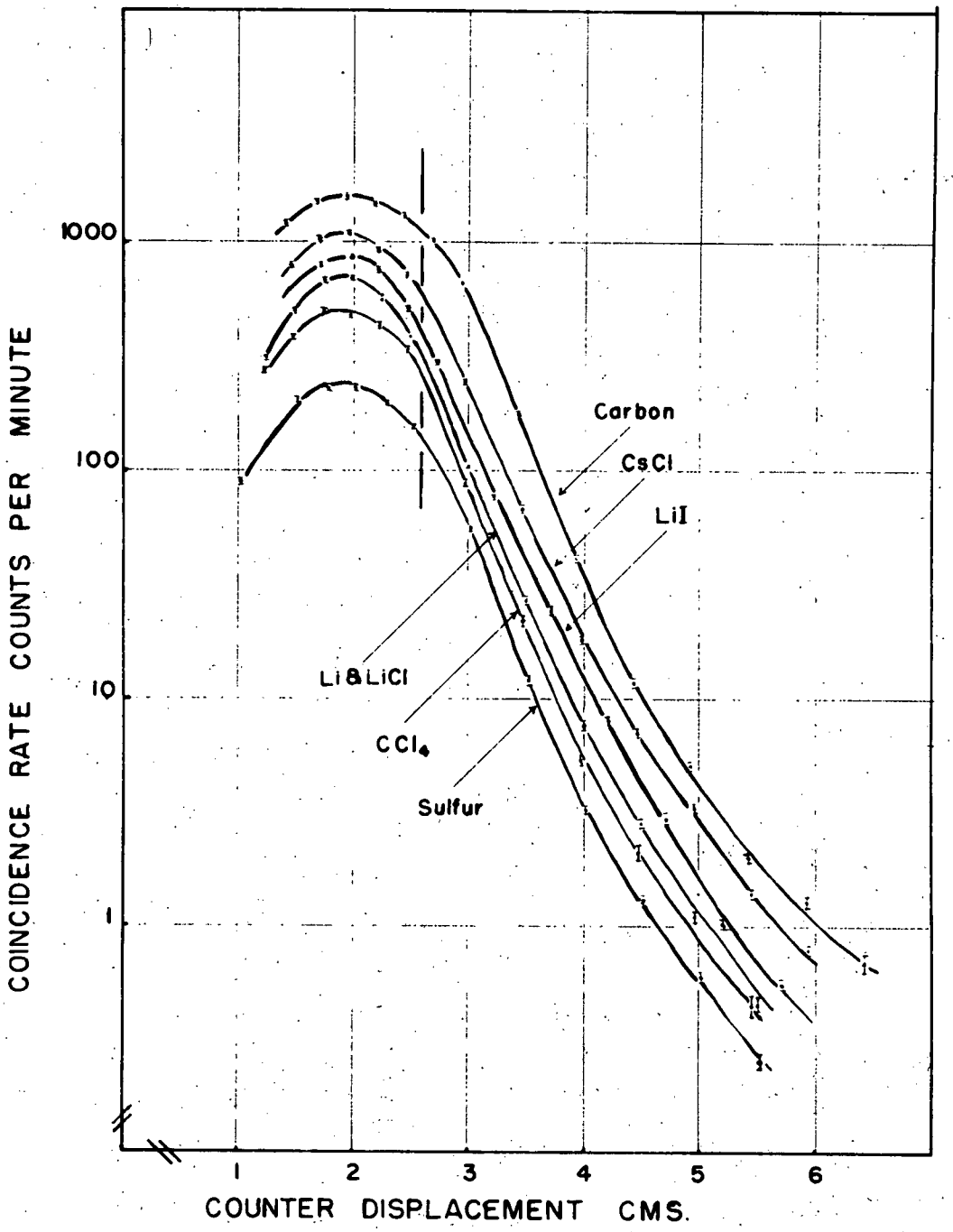

Fig. XII Angular Correlation for Annihilation in C, CCl_4, S, CsCl, Li, LiCl, LiI

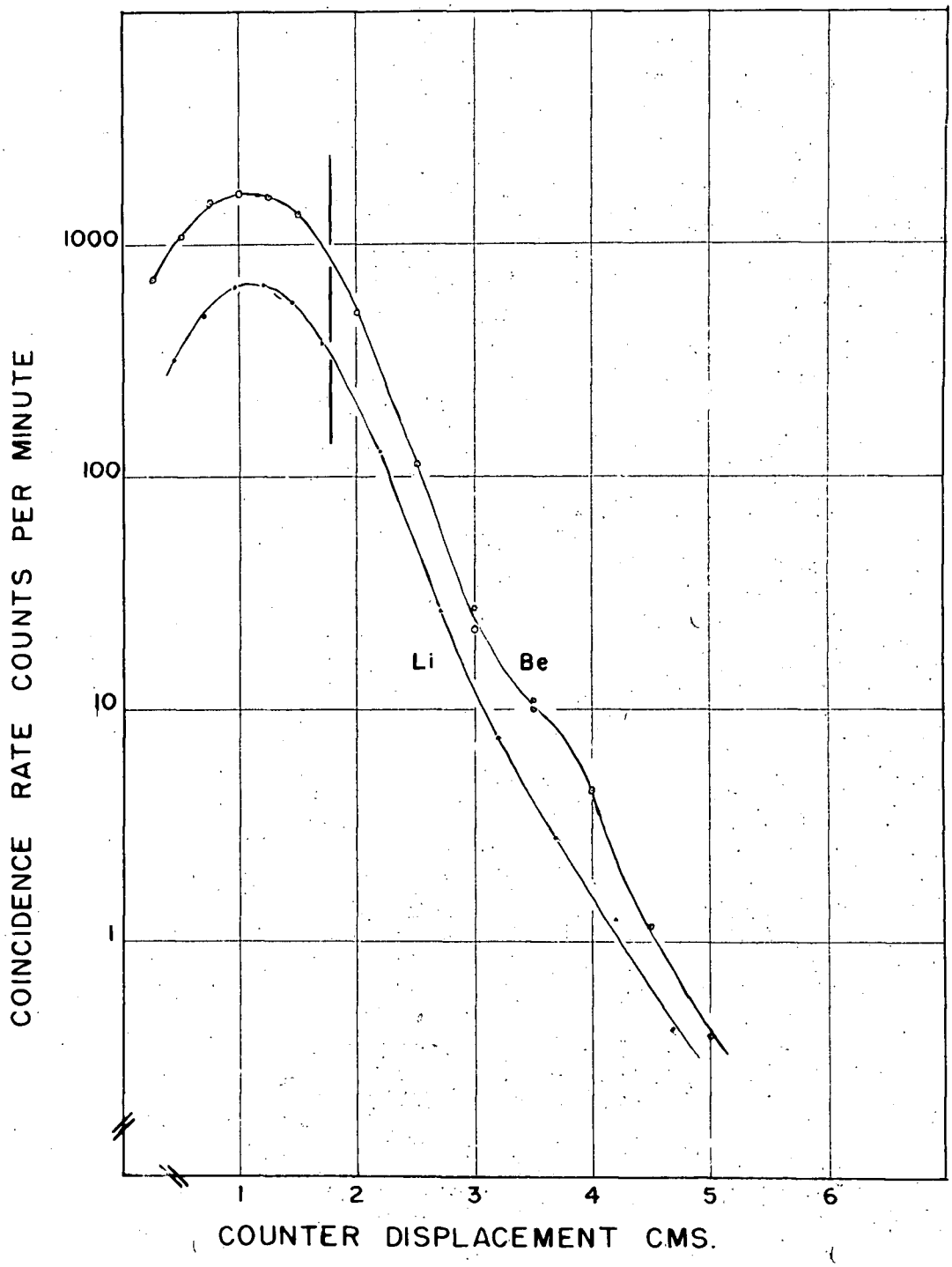

Fig. XIII Angular Correlation for Annihilation in Li and Be

Absorber	Z	A	ρ	θ_o	Av. p	Av. E
Li	3	7	.53 $\frac{gms.}{cms.^3}$	$2.6 \cdot 10^{-3}$	$5.2 \cdot 10^{-3}$ mc	10 e.v.
Be	4	8	1.8	2.3	4.6	8
C	6	12	2.3	2.5	5.0	9
Mg	12	24	1.7	3.0	6.0	14
Al	13	27	2.7	2.4	4.8	9
S	16	32	2.0	2.4	4.8	9
Fe	26	56	7.9	3.4	6.8	18
Ni	28	58	8.9	3.4	6.8	18
Cu	29	63	8.9	3.8	7.6	22
Ag	47	107	10.5	3.3	6.6	17
Cd	48	112	8.7	3.3	6.6	17
Sn	50	118	7.3	3.3	6.6	17
Au	79	197	19.3	3.3	6.6	17
Pb	82	208	11.4	3.2	6.4	15
U	92	238	18.6	2.7	5.4	11
LiCl			2.0	2.7	5.4	11
LiI			3.5	2.7	5.4	11
CsCl			3.9	2.7	5.4	11
CCl_4			1.6	2.7	5.4	11
Teflon			2.0	2.9	5.8	13

Fig. XIV Average Momenta of Mass Centre
(from first three half lives)

N_c/θ curve on some property of the absorber. The thickness of the absorber in each case was the mass thickness required to stop the positrons completely within it. Since the source assembly was turned through a small angle as previously mentioned, the source width was constant for all the materials except for absorbers of very low density such as lithium. The geometrical regions of overlap of source and counters are marked on all curves. The results are displayed in Figures XI, XII, and XIII.

Statistics varied from 2% on the peaks of the curves to 6% at the tails. The counting rates were not normalized to source strength as their display would then have been very confused. A normalization to source strength plus a correction due to photoelectric absorption of 0.51 Mev. quanta, which is as great as 50% in the heavier elements for the thickness of absorber used, yields a superposition of the peaks of the curves.

It is immediately obvious that a "good" exponential type of dependence of the logarithm of the coincidence rate with angle is not a general rule. Groups of materials do have the same general shape.

A group of metals of different electronic shell structure but having a similar N_c/θ dependence is displayed in Figure XI. Due to the shape of the curve the average momentum for a dependence of this type was based on an average exponential slope over the first three half lives.

Curves for a number of metals, salts and co-valently bound compounds are displayed in Figure XII. There is no pronounced

dependence on chemical binding or lattice structure. Certainly the proposed theory[2] of variation with negative ion change as in going through a series of salts such as LiCl to LiI is not borne out.

An anomalous curve (Figure XIII) was obtained for beryllium. There appears to be an inflection in the N_c/θ curve for a beryllium positron absorber at an angle of 1.1°. The energy of pairs giving this inflection would be 130 ev.

Thus, to summarize:

(i) No curves with the exception of copper and teflon appear to be simple exponentials,

(ii) The table (Figure XIV) of values for $p_{av.}$ and $E_{av.}$ from the slopes of the curves immediately outside of the geometrical overlap region shows no correlation with the density or atomic number. The slopes, as mentioned before, are average slopes over the first three half lives of the curves,

(iii) Most curves are markedly similar, particularly in the tails.

V. DISCUSSION

It is considered that these measurements are sufficiently accurate to have shown variations in average electron momenta in various compounds if the current ideas of such momenta are correct and if positrons do reach "thermal velocities" before annihilation. In view of the short lifetime of positrons in solids as measured by both Deutsch[12] and Bell[13], it seems unlikely that such a complete thermalization process as postulated by De Benedetti et al. does occur. It seems more likely that the distribution of momenta observed is that of the positrons which have slowed down in the lattice.

An attempt to explain these results might be aided by a measurement of the N_c/θ dependence through a change in state (liquid to crystalline solid). The mean energy of the electrons should be different in these two cases and possible diffraction effects may also be present. It would also be of interest to see if there is a variation in materials such as amorphous and crystalline quartz that exhibit a change in the lifetime of the positron.

PART II

THE PHOTODISINTEGRATION OF NEON

I. INTRODUCTION

(a) Photonuclear Reactions

The photodisintegration of a nucleus was first achieved by Chadwick and Goldhaber[8] in 1934. They succeeded in splitting the deuteron into a proton and a neutron by irradiation with sufficiently-energetic gamma rays. Other examples of this type of process[17,18,19,20,21,22,23] have been discovered since that time. The threshold energy or minimum energy required to produce the reaction is simply the energy equivalent to the binding energy of the particle which is ejected. The cross section or probability of occurrence of such a reaction is important in the study of nuclear forces.

(b) Photo-Alpha Processes

In the region of low Z in the periodic table, models have been postulated for certain nuclei (Be^8, C^{12}, O^{16}, Ne^{20}) which consist of groups of alpha particles bound together in a geometrical way[15]. This hypothesis is based on the fact that the binding energy per nucleon in an alpha particle is about 7 Mev., a large proportion of the mean binding energy per nucleon for

nuclei of low mass, and if the nucleons are grouped in alpha particle configurations the alpha particles will be bound rather loosely to each other. Thus evidence for a tetrahedron type of configuration for O^{16} has been obtained in angular correlation measurements made by Barnes, French and Devons[16] on the $F^{19}(p\alpha\gamma)O^{16}$ reaction. The corresponding model for the Ne^{20} nucleus is a bi-pyramid of alpha particles, and in this case one would expect that excitation could result in the splitting off of one of the alpha groups.

Another prediction of the alpha particle model is that there are few low-energy excited states in the nuclei investigated. A photo-alpha reaction in $Neon^{20}$ might also give rise to several groups of alpha particles of different energies corresponding to transitions to excited levels in O^{16}. This should in principle allow relatively low excitation levels in O^{16} to be found, if such exist.

(c) Methods of Investigation

Photodisintegration processes will in general have low cross sections of 10^{-27}cm.^{2} or less due to the weak electromagnetic interaction existing between photons and nuclei. Methods involving high sensitivity of detection and large fluxes of gamma rays must therefore be used. (γ, α) reactions in C^{12} and O^{16} have been observed in photographic emulsions. Unfortunately, it would be extremely difficult to introduce Ne^{20} nuclei into an emulsion. Photo processes involving unstable products have been investigated by betatron irradiations, but direct measurements are made with

difficulty due to the high background from these machines. Moreover, the gamma spectrum from them is "white" and interpretation is therefore correspondingly confused. Ionization chamber methods seem suited because neon is a gas having good electron collection properties, and so the photo-alpha disintegration process has been investigated using a gridded ion chamber.

(d) Theoretical Estimate of the Cross Section

Preston[24] has published a summary of a theoretical analysis of the $O^{16}(\gamma,\alpha)C^{12}$ reaction in which an alpha particle model has been used. The results are sufficiently general that an extension can be made to the (γ,α) reaction in Ne^{20}. By a study of unpublished results of Millar and Cameron for the $O^{16}(\gamma,\alpha)C^{12}$ reaction and the results of Goward, Telgedi and Wilkins[25], Preston concludes that since the cross section peaks sharply at an energy well above the Coulomb barrier, the alpha particle may be treated as a plane wave leaving the nucleus and a Coulomb penetrability factor may be applied at lower energies. The wave function of the initial nucleus is written as $\phi_0(r)\psi_0$, where $\phi_0(r)$ is a function of the co-ordinates of the ejected alpha particle and ψ_0 is the wave function of the remaining group. Preston also assumes that the gamma interaction must be quadrupole, due to symmetry, and so obtains matrix elements of the form

$$\int \psi_f^* e^{\frac{i\bar{p}\bar{r}}{\hbar}} x z \phi_0(r) \psi_0 \, d\tau$$

for the transition probability of the reaction, where $e^{\frac{i\bar{p}\bar{r}}{\hbar}} xz$ is one of the terms for the quadrupole interaction

of the photon with the ejected alpha particle, and ψ_f is the wave-function of the residual nucleus. He assumes that considerable overlap occurs between the wave-function of C^{12} and the residual wave-function in O^{16} in which case the approximation can be made $\int \psi_f^* \psi_0 \, d\tau \approx 1$. A specific reference to O^{16} is lost at this point and only an upper limit can be set on the cross section by evaluating the remaining matrix elements. For $\phi_0(r)$ Preston uses:

An exponential function $e^{-\frac{r}{b}}$

A Gaussian function $e^{-\frac{r^2}{b^2}}$

A modified Wheeler function $e^{-\frac{r^2}{b^2}} f(r, a/b)$

a and b are parameters in the function which give a maximum cross section at the gamma ray energy at which it is experimentally observed, i.e. 17 Mev. However, the results are not markedly different, in the case of the Wheeler function, from the Gaussian. This last assumption, together with the estimate that the overlap of ψ_f and ψ_0 for the $Ne^{20}(\gamma, \alpha)O^{16}$ should be about the same as in the $O^{16}(\gamma, \alpha)C^{12}$ case, immediately leads to the conclusion that the two cross sections should be of about the same order of magnitude. The use of the modified Wheeler formula would tend, however, to change the value of the gamma ray energy for which the maximum cross section occurs.

The threshold energy for the $Ne^{20}(\gamma, \alpha)$ process is 4.6 Mev., as calculated from mass values; that of the $O^{16}(\gamma, \alpha)$ is 7.2 Mev. If a nuclear radius of 5×10^{-13} cms. is used the Coulomb barrier

height is 6.1 Mev. for the Ne^{20} reaction but only 5.0 Mev. in the latter case. The threshold plus Coulomb barrier height corresponds to 10.7 Mev. for neon. Any gamma ray of lower energy would therefore have a decreased probability of interaction due to the penetrability of the Coulomb barrier. It is interesting to note that the total energy required in the case of O^{16} is 12.2 Mev. which would lead to the speculation that, with the gamma ray energies above this barrier plus the threshold level, the $Ne^{20}(\gamma, \alpha)$ cross section should be of about the same size as the O^{16} threshold or perhaps a little larger if the previous argument about overlapping wave-functions is reasonable.

(γ, α) reaction cross sections have been measured in the case of O^{16} by Waffler and Younis[26] who report a cross section of $(1.8 \pm 0.6) \times 10^{-28}$ cm.^{2} for $O^{16}(\gamma, \alpha)C^{12}$ with gamma rays of 17.6 Mev. energy and in the case of C^{12} by Goward, Telgedi and Wilkins[25] who report a cross section of 10^{-28} cm.^{2} for $C^{12}(\gamma,\alpha)Be^{8*}$ $Be^{8*} \rightarrow 2He^4$ with gamma rays of 18 Mev. energy at the maximum cross section. The cross section for the reaction $Ne^{20}(\gamma, \alpha)O^{16}$ would therefore be expected to be of the same order of magnitude.

(e) Purpose of Present Experiment

Since there is a considerable controversy as to the mechanism involved in a photodisintegration process and a previous experiment by Woods[27] seemed to indicate an unexpectedly low cross section for the (γ, α) process in Ne^{20} (less than 10^{-29} cm.^{2}) it was felt worthwhile to examine this reaction again with refinements in technique which would allow a cross section of 1×10^{-30} cm^2. to be detected with certainty.

II. THE EXPERIMENTAL TECHNIQUE

(a) General Considerations in Cross Section Measurements

A reaction cross section may be defined by the equation

$Y = \sigma nN$.

Y = yield of the reaction per unit time

σ = cross section of the reaction occuring

N = number of nuclei in the target capable of taking part in a reaction which can be detected

n = number of bombarding nuclei per unit area per unit time

Thus the determination of a cross section consists of two parts: one the measurement of the yield of the reaction, and the other the measurement of the flux of the bombarding particles, or quanta, as the case may be. The number of effective target nuclei is usually easily found.

For the $Ne^{20}(\gamma, \alpha)O^{16}$ reaction a gridded ionization chamber was chosen as a detector and a sodium iodide crystal mounted on a photomultiplier was used to measure the absolute magnitude of the gamma ray flux which was obtained by the bombardment of a thick lithium metal target with protons from the University of B.C. Van de Graaff generator.

(b) The Ionization Chamber

The passage of a proton, an alpha particle, or heavier charged particle through a pure, inert, rare gas produces electron and positive ion pairs in number closely proportional to the kinetic energy of the particle. Hence by arranging a suitable electrostatic field, the whole of the electrons may be collected on a positive electrode, giving rise to a voltage pulse at the electrode, the amplitude of which is proportional to the total energy released by the ionizing event. The details as to the shape and formation of this pulse have been discussed by Wilkinson[28] and Woods[27].

In normal two-electrode chambers the pulse has a slow rise time due to the space charge of positive ions which have a low mobility compared to the electrons. To remove the slow rise due to this positive ion effect and hence allow the use of an amplifier with a much narrower band pass, Frisch[29] has suggested that a third electrode or grid be placed in front of the collector. The pulse rise time is then dependent only on the electron collection time from the moment the first electron passes the grid. The position of the grid for most effective shielding has been investigated by Bunemann, Cranshaw and Harvey[30].

A series of experiments[31,32,33,34] in various types of ion chambers containing argon gas has shown that W(the energy loss per ion pair on the average) is nearly a constant for various alpha particle energies. This allows quantitative energy measurements to be made because a natural alpha source of known energy can be used to give the energy calibration of a chamber.

Wilkinson[28] has also determined that a high purity of gas is necessary (as little as 1 part in 10^5 of oxygen, an electronegative gas, in argon at atmospheric pressure will capture one percent of the liberated electrons in 6 cm. of motion and this effect increases rapidly with pressure). Because of the release of occluded gases a continuous purification is necessary.

(c) Source of Gamma Rays

A monochromatic source of gamma radiation of energy above 10.7 Mev. in energy was required for the experiment in order to raise the Ne^{20} to a high-enough excitation that alpha particles could be emitted with an energy greater than that of the potential barrier. Of the gamma rays produced in nuclear reactions, two suggested themselves:

(1) $H^3 + p \longrightarrow He^{4*} \longrightarrow He^4 + \gamma$ (20 Mev.)

(2) $Li^7 + p \longrightarrow Be^{8*} \longrightarrow Be^8 + \gamma$ (17.6 Mev.)

$\longrightarrow Be^{8*} + \gamma$ (14.8 Mev.)

The tritium reaction has not yet been used since the gamma-ray yield from the zirconium-impregnated targets available appears to be much lower than that from the lithium reaction.

Two groups of gamma rays are emitted in the Li(p, γ α) reaction, of which only the 17.6 Mev. gamma ray has a narrow, line energy spread (about 12 Kev.[35]). The 14.8 Mev. gamma ray is actually a spectrum with an energy width of 2 Mev. which arises from the transition from the excited state at 17.6 Mev. to the broad excited state of Be^8 at 2.9 Mev. The reaction has been

studied in detail by Walker and McDaniel[36] and cross sections for the production of both the 14.8 and 17.6 Mev. gamma rays using a thick lithium metal target with various energies of bombarding protons have been given by them. There is also a slowly rising non-resonant yield in this reaction which allows the gamma-ray energy (at bombarding energies of protons greater than the 440 Kev. resonance) to be varied by changing the bombarding energy. The cross section for this non-resonant yield is much lower than the resonant cross section and the gamma ray contribution from it is small.

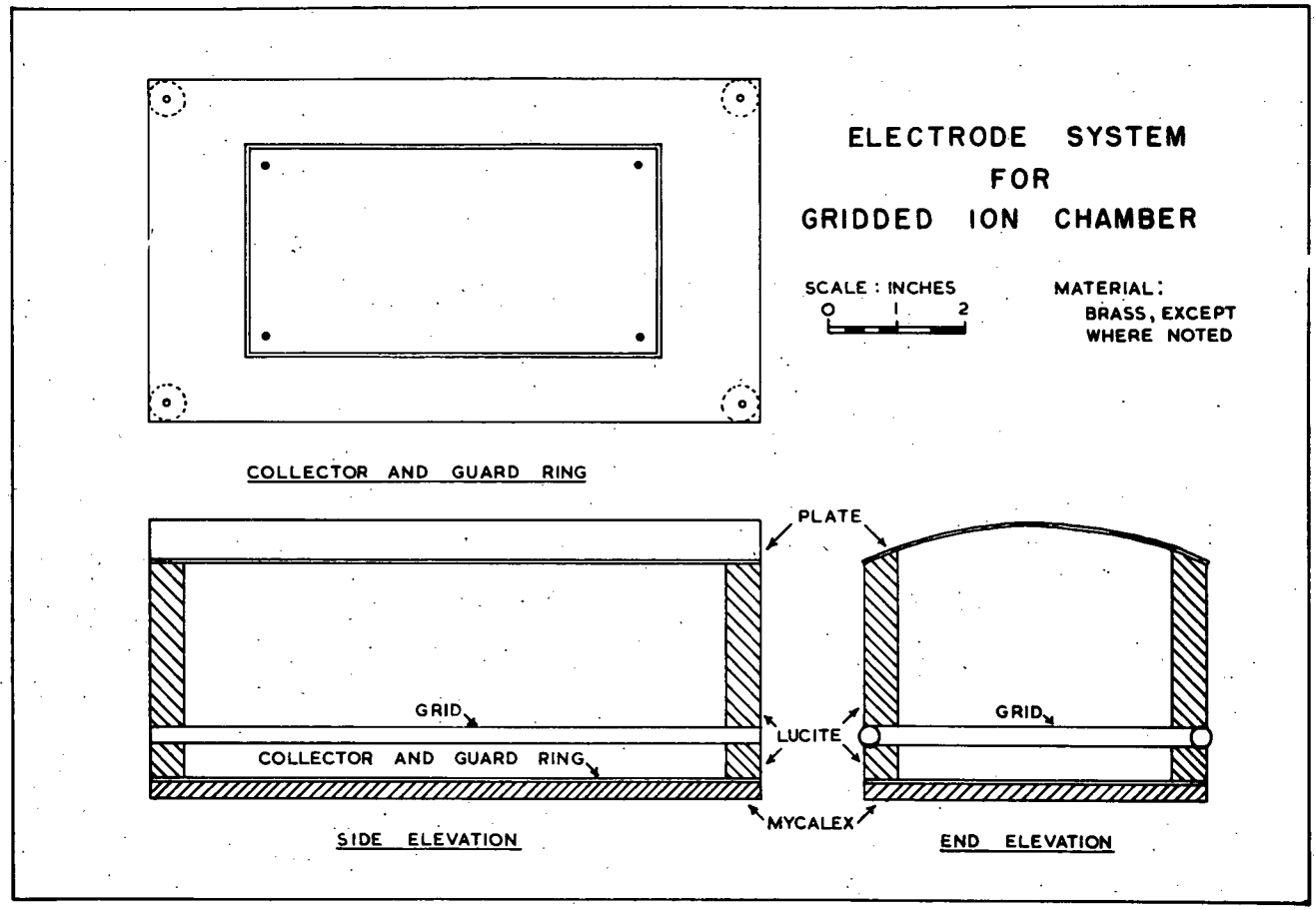

Fig. XV Electrode System of Ion Chamber

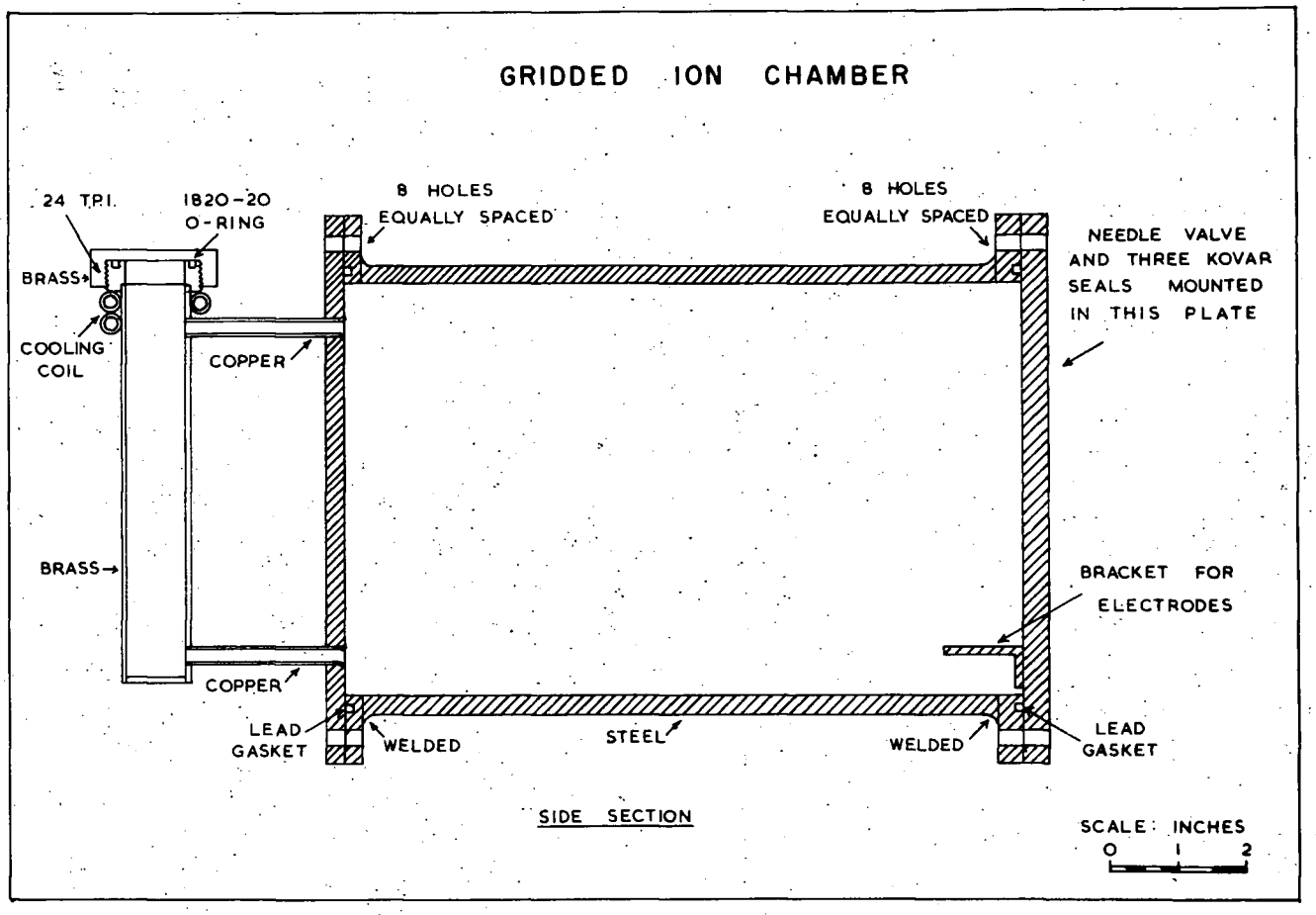

Fig. XVI Outside Casing of Ionization Chamber

III. THE EXPERIMENTAL ARRANGEMENT

(a) Gridded Ion Chamber (Figure XV)

The chamber was constructed according to the formulae given by Bunemann et al[30]. The electrode structure was contained in a seamless steel tube (Figure XVI), 6 inches in diameter and 10 inches in length with a $\frac{1}{4}$-inch wall thickness. $\frac{1}{4}$-inch thick end plates were bolted to welded flanges and the seal was accomplished with lead gaskets to prevent exposure of the filling gas to rubber. The chamber was painted with colloidal graphite on all the internal surfaces to reduce the background of natural radioactivity from the walls and to reduce the effect of (γ,ρ) processes.

The gas purifier was carried on one end plate. It was of the type used by Jentschke and Prankl[37] and described by Wilkinson[28], and was connected to the chamber by two copper tubes. It consisted of a brass tube 6 inches long and one inch in diameter around which a heater coil was wound which was capable of raising the temperature to 300°C. The inside was filled with turnings of calcium metal which readily forms solid compounds with gases such as oxygen and nitrogen above 220°C. and should take out water when cold. The opposite end plate supported the electrode struc-

ture, the kovar seals by which electrical connections were made to the H.T. voltage and amplifier, and the valve by which the chamber was filled.

The electrodes were of brass with mycalex and lucite insulation, the grid being of #36 Copel wires spaced 1 m.m. apart on a brass frame. The high voltage electrode was curved, to increase the number of lines of force arriving at the collector, in a fashion determined by measurements made in an electrolytic tank. The collector, 6 inches by 3 inches, was surrounded by a guard ring $1\frac{1}{2}$ inches in width. The grid was 0.6 inches from the collector and 3 inches from the high voltage electrode. With these dimensions the grid inefficiency or the extent to which the number of lines of force ending on the collector is dependent on the field of the positive ions was 1%.

The voltages recommended by Bunemann et al[30] were not quite suitable for the chamber with neon gas. From observation of the pulse height as the grid voltage was changed, it was decided to work with Vg = 0.45 Va. The high voltage electrode was run at 800 volts. The pulse height increased in size until -700 volts was reached and then remained constant until -900 volts at which time breakdowns occurred in the neon due to its known poor electrical quality.

The chamber contained pure neon gas at a pressure of 473.5 cm. of mercury or 6.25 atmospheres. The choice of gas pressure was made so that the range of the alpha particles should be kept small (3 cm.) to keep the wall effect low for the high energy groups expected (10 and 13 Mev.). The high-energy incident gamma quanta are well above the threshold for the gamma-p processes and

at this pressure the maximum energy which may be dissipated by a proton in the sensitive volume is 7.8 Mev. Since no proton of higher energy can liberate more than 7.8 Mev. and the chamber was filled with neon gas (containing Ne^{20}, Ne^{21} and Ne^{22} in abundances of 90.51%, 0.28%, and 9.21%[61]) only (γ, α) reactions in the neon can produce pulses above this level.

Filling was accomplished by passing the compressed gas of a high purity (He 0.02%; N 0.02%; others less than 0.02%) through a liquid nitrogen cold trap and directly into the chamber. The resulting pressure was obtained from the equalization of the pressures in the chamber and filling bottle. Electron collection was obtained with no difficulty but the heater was run for some time and the pulse size increased slightly.

(b) Electronics and Pulse Analysis

The head amplifier was the low-noise model 500 type of Elmore and Sands[40]. A cathode follower fed the pulses from this amplifier, which had a gain of 100, down a 100 ohm cable properly terminated at the main amplifier.

The main amplifier was a Northern Electric Type 1444 amplifier with a maximum gain of 10^4 and a stability of better than 1% over long periods. The differentiation and integration time were both set by the controls available on this instrument, to 5 microseconds. At 6 db attenuation the 5.29 Mev. alpha peak from Po^{210} was 26.2 volts in amplitude.

The voltage distribution of the amplified pulses was measured by feeding them into an 18 channel "pulse amplitude analyzer" or "kicksorter", designed by Westcott and Hanna[41] and built accord-

ing to specifications of the National Research Council of Canada, Chalk River Laboratory, by Canadian Marconi Ltd..

The discriminators determining the voltage intervals were set from a precision pulse generator designed by Bowers[42]. Its output was stable to 0.01 volts over long periods of time. The kicksorter unit has a stated amplitude stability of less than 0.02 volts. This was found to be the case by a 24-hour check with the pulse generator.

The linearity of the equipment was determined by feeding pulses of calibrated amplitude through a potentiometer into the grid of the ion chamber and measuring the output voltage level for various input pulse amplitudes. The linearity of the electronic system was found to be better than 1%.

The energy scale was determined by a Po^{210} alpha source which was fastened to the inside of the high voltage electrode and gave about 3 alpha particles per minute. The range of 5.3 Mev. alpha particles in 6.25 atmospheres of neon is about 1 cm., so all of the alphas were stopped in the sensitive volume. A typical alpha particle pulse distribution is shown in Figure XVI. The width of the pulse spectrum is largely due to amplifier noise as was seen by the comparison with a standard pulse spectrum, which was produced by feeding pulses from a pulse generator into the grid of the head amplifier. The small extra width is due to straggling in ionization and source thickness.

All the amplifiers, power supplies and the H.T. voltage were supplied from regulated 110 volts A.C. obtained from constant voltage Sola transformers loaded to at least 85% of their rated load. The Solas were isolated from the mains with filters to

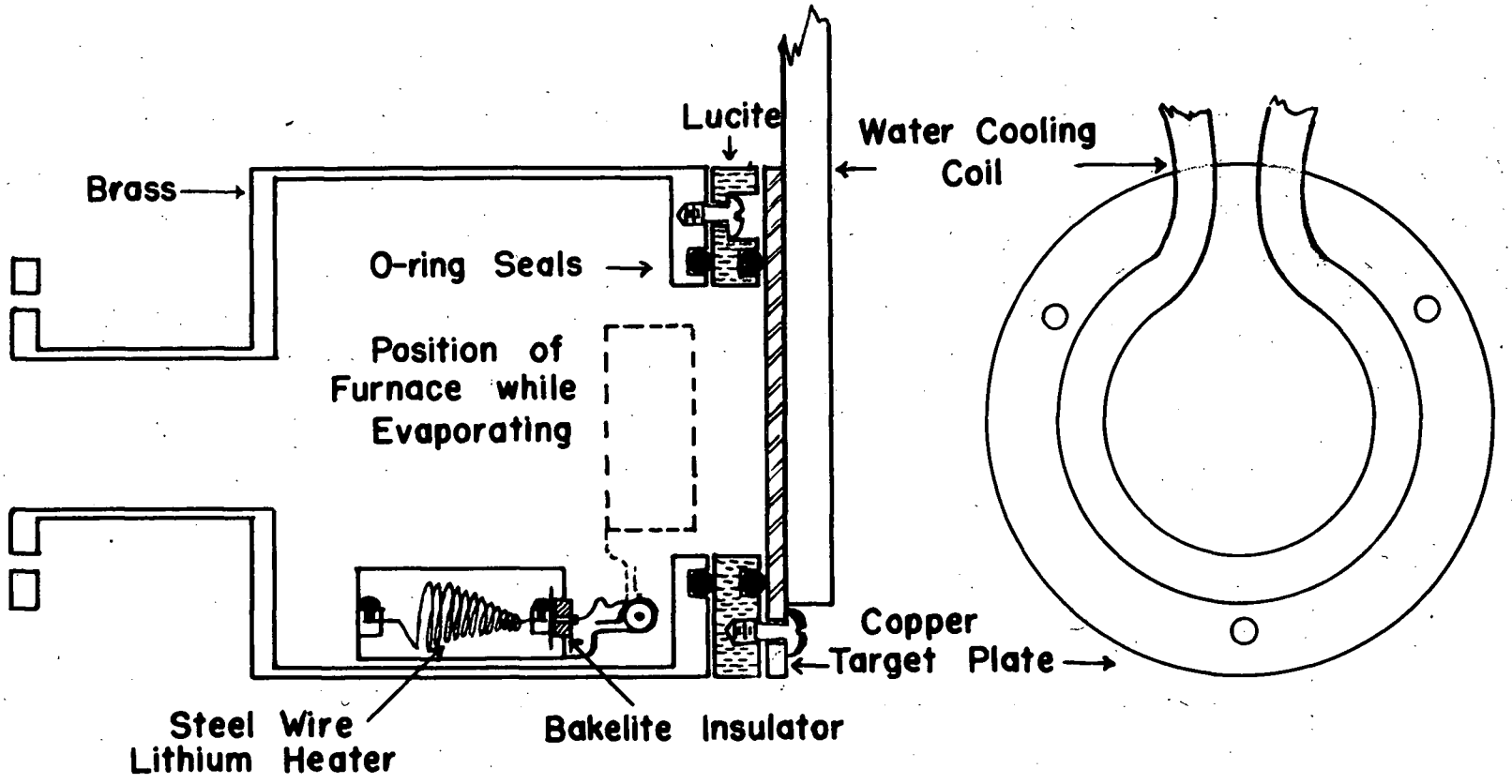

Fig. XVII Lithium Metal Target Evaporating Chamber

prevent spurious line pulses from entering the equipment.

(c) Lithium Target Arrangement

A target chamber was constructed for evaporation of lithium metal under evacuation. This system is shown in Figure XVII. The lithium metal was placed in a heater of spiral spring steel wire. The system was evacuated and the shutter was closed to the main system. The heater was turned on and a lithium metal layer was evaporated on the 1/8-inch thick copper end plate. The water cooling coil of copper tubing was hard soldered to the periphery of the plate to give a minimum mass thickness of absorber between the source of the gamma rays and the ionization chamber. The thickness of the targets used was about 700 Kev., as determined from the gamma ray excitation function (e.g. Figure XVIII).

(d) Gamma Ray Flux Determination

The flux of gamma rays was determined in two ways to give a check on the integrated number of gamma rays passing through the gas in the sensitive volume of the ionization chamber.

In the first place, the integrated proton current to the target was measured and the flux calculated from cross section data. The $Li^7(p,\gamma)$ cross section has been accurately measured by Walker and McDaniel[36] with a pair spectrometer, and has been given for various bombarding energies of protons on thick lithium targets. The copper plate on which the target was fastened was held at a potential of +300 volts with respect to the evaporating chamber and so the integrated proton current to the target could be expected to be very closely the true current of protons,

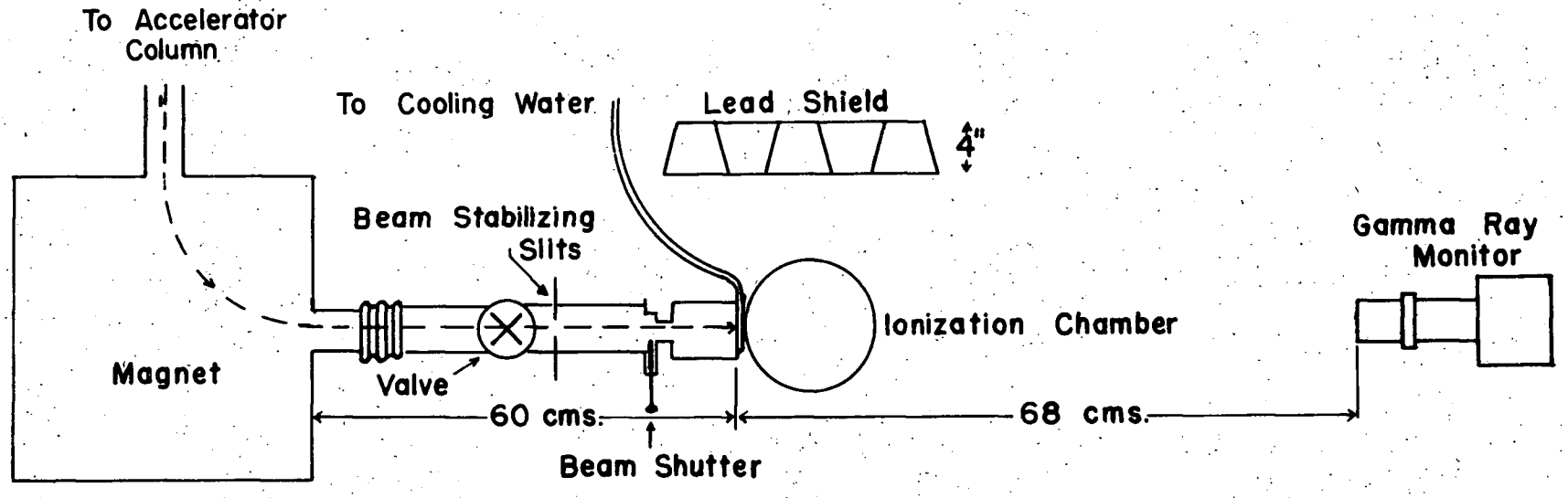

Fig. XIX Experimental Arrangement for Photodisintegration Measurement

since the chamber acted as a Faraday cage preventing electrons from being boiled off the target by secondary emission effects. The Walker and McDaniel cross section ratios were extrapolated to the bombarding energy of 650 kilovolts used in the experiment, since the shape of the thick target excitation function was known (Figure XVIII). The flux of gamma rays at the target was calculated using the integrated current and the extrapolated cross sections.

Secondly, absolute measurements of the flux were made with a photomultiplier and large NaI(Tl) crystal. The crystal, 4.46 cm. in diameter and 5.08 cm. in length, which was mounted on the end of an E.M.I. 6262, 14-stage photomultiplier, according to the method of Swank and Moenich[43], was used as the gamma ray detector. The mounting method has been further developed and modified by Griffiths[45] and Azuma[44]. The total gamma ray flux was calculated* (Appendix II) from the shape of the observed gamma ray spectrum and the counting rate obtained from the crystal with the discrimination level set at a pulse height corresponding to 10.5 Mev. The pair production cross section as well as the cross section for Compton effect given by Heitler[1] were used in the flux calculation. Pair production in the field of the electrons and the effect of the thallium, activating impurity has been neglected but would only contribute a very small correction of the order of 1% or 2%.

The target chamber and gamma ray monitor were mounted in a direct line (Figure XIX). The chamber was removed to measure the flux from the target alone and then was inserted to give an absorption measurement for the chamber walls. Repeated readings

---

* I am indebted to G.M. Griffiths for his aid in making the flux determination.

of this absorption correction agreed to within 2%.

The gamma-ray flux calculated by the scintillation counter method and the flux calculated by the cross section and integrated current method agreed to within 10% in a two-hour bombardment of the target at the beginning of the experiment. The agreement became worse during the course of the experiment due to the deterioration of the target, but at no time was it worse than 20%.

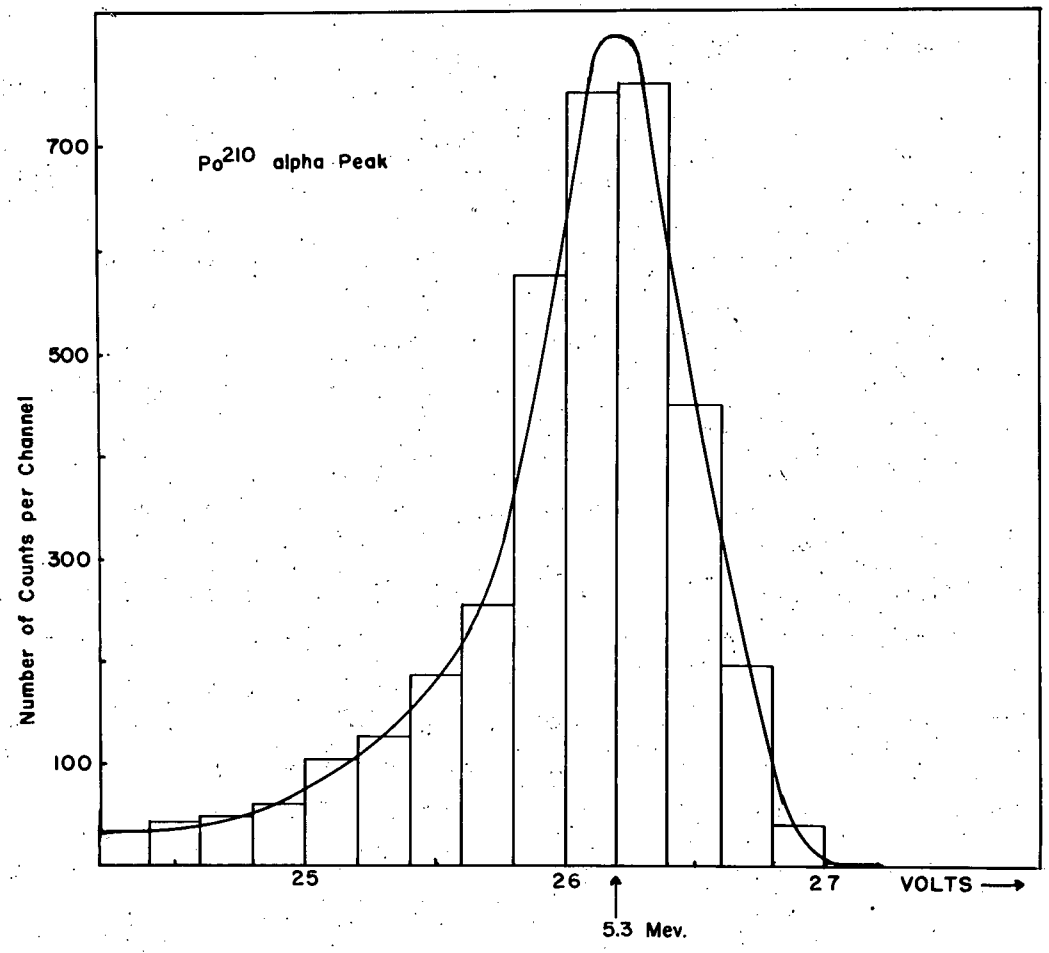

Fig. XX Po^{210} Alpha Peak

IV. EXPERIMENTAL PROCEDURE

(a) Energy Calibration

The ionization chamber was connected via the Northern Electric amplifier to the kicksorter and a run was taken on the Po^{210} alpha peak (Figure XX) to calibrate the voltage scale from the known alpha energy (5.29 Mev.) and to check the stability of the amplifiers. At the attenuation of 12 db on the Northern Electric amplifier this peak appeared at 13 volts. The kicksorter was set up to cover the energy range from 5 Mev. to 14 Mev. in 530 Kev. energy steps (530 Kev. was equivalent to 1.30 volts width per channel). To give a quick check on the stability during the course of the experiment, pulses from a standard pulse generator were fed on to the collector of the ionization chamber. This was necessary as the specific activity of the Po^{210} calibrating source was low.

The gamma ray monitor counter output was fed via an Atomic Instruments Company 204C amplifier and discriminator to a scaler. In order to set the discriminator bias to an energy level corresponding to pulses produced in the crystal due to a 10.5 Mev. energy loss, the energy at which the bias was set in the calibration run for the gamma ray monitor, an energy scale was set

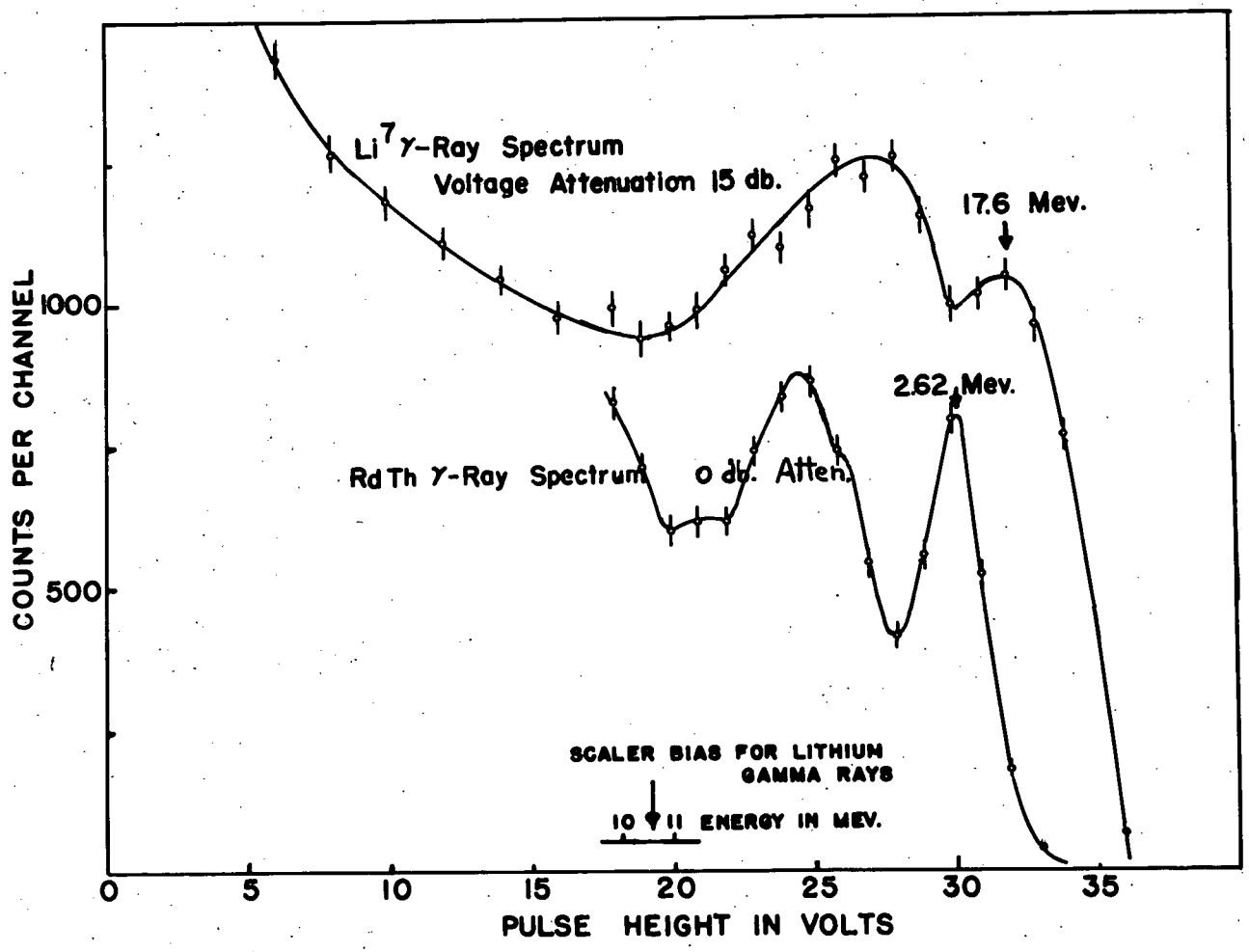

Fig. XXI Li(p,γ) Gamma Ray Spectrum

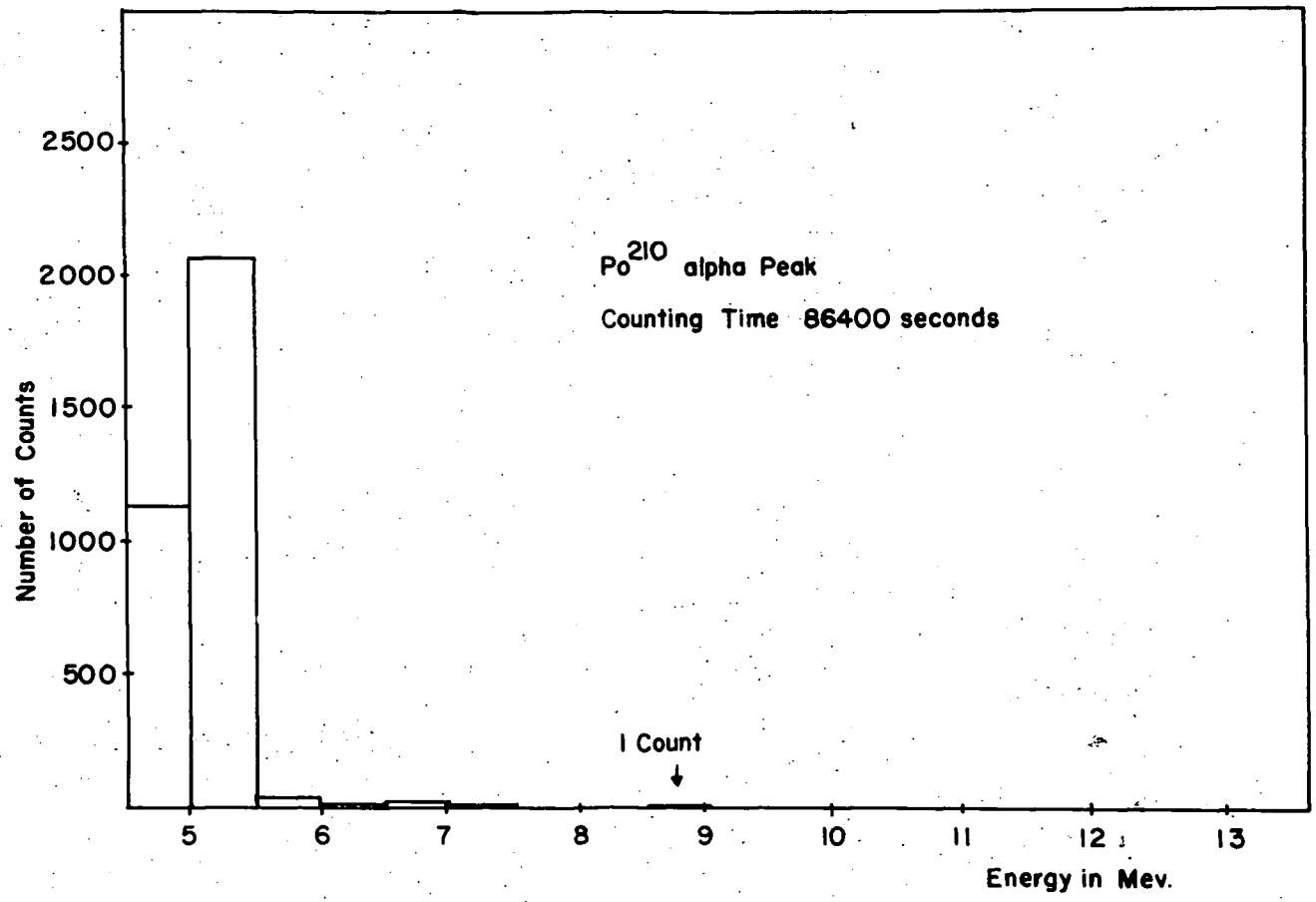

Fig. XXII Background in Ionization Chamber with Accelerator off

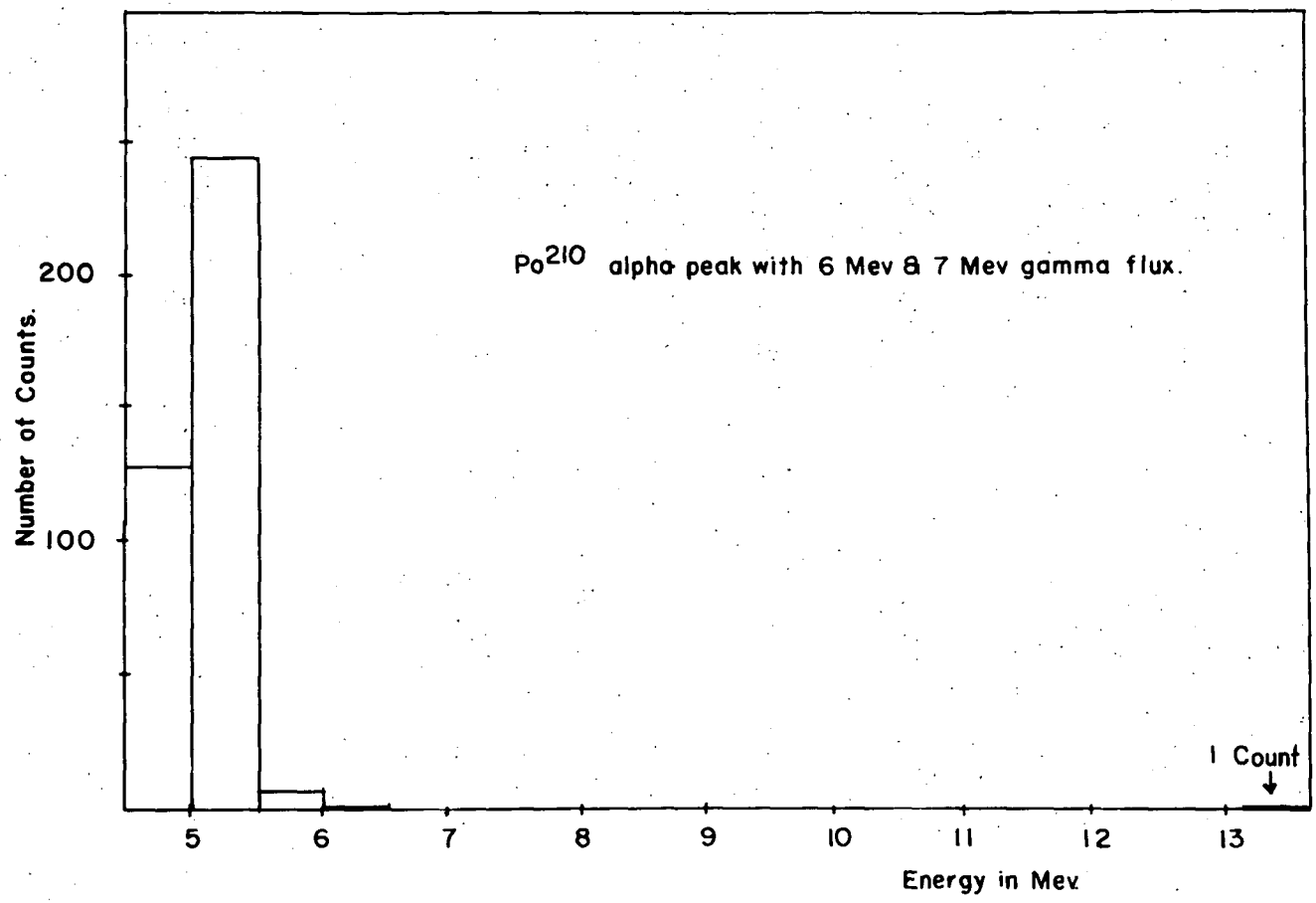

Fig. XXIII Background in Ionization Chamber Bombarded with Fluorine γ-rays

up using the 2.62 Mev. Th C" gamma rays. The gain was reduced by a factor of 4 and the bias was re-adjusted to correspond to a discriminator level of 10.5 Mev. The two spectra are shown in Figure XXI. The bias level was checked at intervals throughout the course of the experiment to ensure the constancy of the monitoring.

(b) Photodisintegration Measurements

A resolved proton beam of 25 microamperes was focussed on the target and the electric timer, current integrator, gamma-ray monitor, and kicksorter were switched on simultaneously from a master relay unit.

Readings were recorded every 15 minutes and once every two hours a complete gain check was made for both the ionization chamber and the gamma-ray monitor.

Measurements on background were made in two ways:

(i) A long count (6 hours) was taken with the chamber in the standard position and no proton beam on the target (Figure XXII).

(ii) A run was made with the proton beam on a calcium fluoride target. This is a prolific source of 6 and 7 Mev. gamma rays and the large gamma flux should produce noise due to "build ups" in the ionization chamber. The results are shown in Figure XXIII.

Finally having established the existence of the reaction the energy spectrum of the disintegrations in the chamber was examined with finer resolution by spreading the spectrum out over the kicksorter so that each channel covered 200 Kev. of energy. In this way an investigation was made of the spectrum in three separate sections in an attempt to ascertain if any fine structure was present.

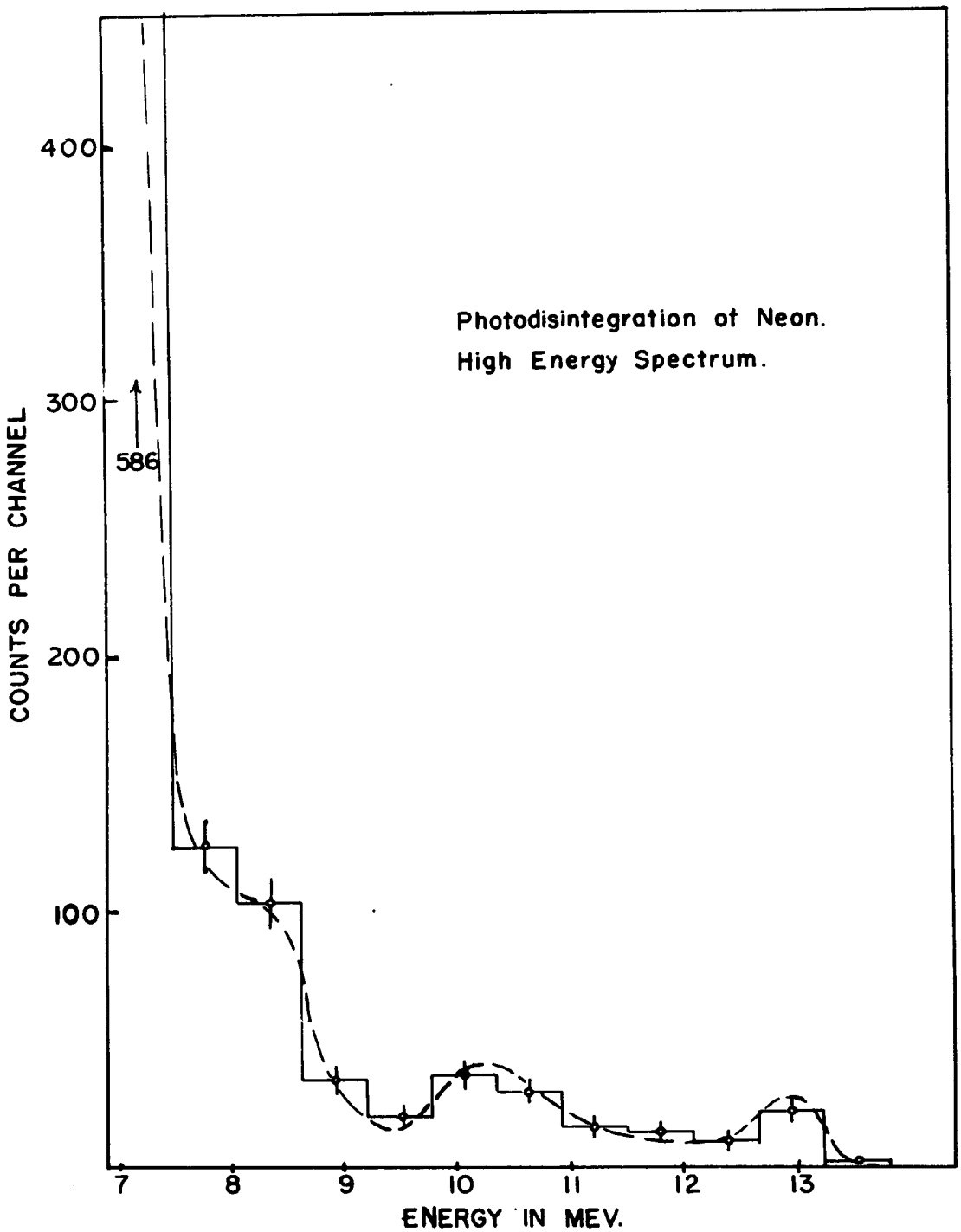

Fig. XXIV Spectrum of Pulses in Chamber above 8 Mev.

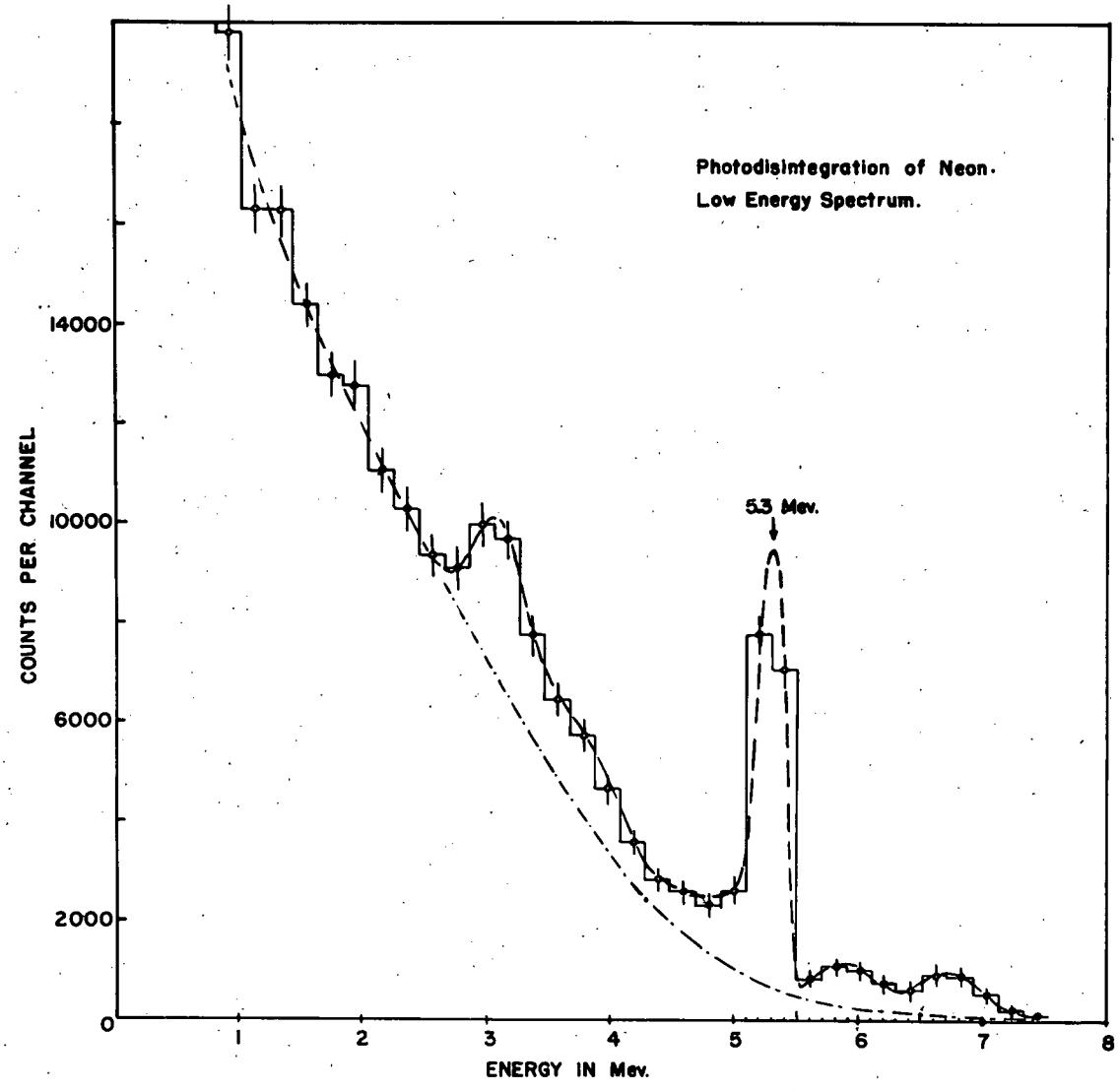

Fig. XXV Spectrum of Pulses in Chamber below 8 Mev.

V. RESULTS

(a) Discussion of Pulse Spectrum

The pulse height distribution on an energy scale is displayed in Figures XXIV and XXV. It is divided into two regions, one below and one above the pulse height corresponding to an energy release of 7 Mev. in the chamber. The two regions are normalized to the same integrated flux of gamma rays.

Peaks may be seen to occur in the distribution at 3.1, 4?, 5.9, 6.8, 8, 10.5 and 12.9 Mev. The background of pulses occurring above the Po^{210} alpha peak was negligible, as shown in Figure XXIII, even when the proton beam was incident on a calcium fluoride target which gave a very large flux of gamma radiation. Since a resolved beam was used in bombarding the lithium target only those neutrons arising from secondary reactions in the target itself could give neutron-induced reactions in the chamber gas or the walls. The maximum neutron energy which can be produced in the secondary $Li^7(\alpha, n)$ reaction, from the low percentage of ground state alpha particles from the excited state of the Be^8 compound nucleus produced by the bombardment of the target with protons, is 5.2 Mev. This could only produce 5.1 Mev.

alpha particles in the chamber via $Ne^{20}(n,\alpha)$ processes, which would give pulses below the alpha peak. A possible $N^{14}(n,\alpha)$ reaction is energetically too low as well, since the Q of this reaction, like that of the $Ne^{20}(n,\alpha)$ reaction, is negative. The possibility of this reaction must be considered due to its high cross section. Furthermore, a measurement made with a ZnS detector (ZnS on the photocathode of a 5819 photomultiplier[62]) with a hydrogenous radiator for detecting high energy neutrons did not give a counting rate which was significantly above its background rate. Measurements made with the same detector in a bombardment of D with protons[45] easily detected the neutrons produced by the "knock-on" deuterons in this experiment. It is concluded, therefore, that no significant flux of high energy neutrons was present, and the pulses in the ionization chamber corresponding to energy release greater than 7.8 Mev. (Figure XXIV) could be justifiably attributed to:

(i) $Ne^{20}(\gamma,\alpha)O^{16}$ ground state from both 17.6 and 14.8 Mev. gamma radiation which give rise to energy releases 12.9 and 10.1 Mev. respectively.

(ii) $Ne^{22}(\gamma,\alpha)O^{18}$ from the 17.6 Mev. gamma ray with an energy release of 8.0 Mev.

The cross sections for the $Ne^{20}(\gamma,\alpha)O^{16}$ reactions can be calculated from the yield figures and are $8.0 \pm 2 \times 10^{-30}$ cm.^{2} for the 17.6 Mev. gamma ray and $3.0 \pm 0.6 \times 10^{-29}$cm.^{2} for the 14.8 Mev. gamma ray. Although the cross sections are stated to 20% accuracy the ratio of the two cross sections can be defined much more exactly from the ratio of the number of pulses in the

two peaks, viz. 117/44. By taking the ratios of 14.8 to 17.6 Mev. gamma radiation according to Walker and McDaniel[36], and extrapolating to the 650 Kev. bombarding energy used in the experiment, a value of .6/1 is obtained for the ratio of these gamma rays. From these two ratios the ratio of the cross sections becomes

$$\frac{\sigma_{14.8}}{\sigma_{17.6}} = 4.5 \pm 1.0.$$

Although the amount of Ne^{22} present in the chamber is known (9%) the cross section for the $Ne^{22}(\gamma,\alpha)O^{18}$ reaction can not be calculated to better than an order of magnitude because the disintegration group is on the edge of a steeply-rising curve due to the (γ, p) background. This cross section is about 10^{-28} cm.^{2}, a value which is not inconsistent with other photodisintegration cross sections.

The energies of the two groups above the Po^{210} alpha peak at 5.9 and 6.8 Mev. (Figure XXV) agree so well with the expected energies of alpha groups to the 7.1, 6.9 and 6.13 Mev. excited states of O^{16} for the reaction $Ne^{20}(\gamma,\alpha)O^{16*}$ (17.6 Mev. gamma radiation) that they may be ascribed to it. The cross section for the reaction to the 6.05 Mev. level of O^{16}, which has the same spin and parity as the ground state, would be expected to be only of the same order of magnitude as the ground state. The energy of the higher alpha group is certainly much closer to 6.7 Mev. than to 6.9 Mev. (bearing out this assumption). By using the mass difference between O^{16} and Ne^{20} as given by Ajzenberg and Lauritsen[48] of 4.75 Mev., the reaction to the 6.05 Mev. level should have a Q of 6.80 Mev. and to the 6.13 Mev. level a Q of 6.72 Mev. It seems likely that the reaction is proceeding

through the 6.13 Mev. state of O^{16}.

The mean Q of the reactions proceeding through the 6.9 and 7.1 Mev. levels of O^{16} is 5.85 Mev. The centre of gravity of this peak is close to this value.

With this interpretation the cross section for the reaction $Ne^{20}(\gamma,\alpha)O^{16*}$ is $4.0 \pm 1.6 \times 10^{-28}$ cm. to the 6.9 and 7.1 Mev. excited states and $3.0 \pm 1.2 \times 10^{-28}$ cm. to the 6.13 Mev. excited state.

An unambiguous assignment can not be made to the peaks in the pulse distribution curve below the Po^{210} alpha group due to the large number of possible (γ, p) processes ($Ne^{20}(\gamma,p)F^{19}$). It is interesting to note that the energy of the peak at 3 Mev. does correspond to the reaction $Ne^{20}(\gamma,\alpha)O^{16*}$ (14.8 Mev. gamma radiation) to the excited states of O^{16} at 6.9 and 7.1 Mev. and the shape of the curve is such that there is also an indication of this same reaction to the 6 Mev. excited states. The cross section for the reaction corresponding to this peak is $1.0 \pm 0.5 \times 10^{-27} cm.^2$.

(b) Cross Section Calculations

The cross sections for the reactions as calculated by the two methods previously described agreed very well. As an example, the cross section calculated for the $Ne^{20}(\gamma,\alpha)O^{16*}$ (17.6 Mev. gamma radiation) to the 6.9 and 7.1 Mev. excited states of O^{16} is treated below.

The yield of the reaction can be obtained from a sum of the counts under the peak at 6 Mev. which lie above the background in Figure XXV. This background was drawn in from the general shape

of the curve and the knowledge that no (γ, p) process in the chamber could give rise to pulses greater than 7.8 Mev. The unknown shape of the background introduces an error into the cross section, but this error can not be greater than 30%. The yield in this case was 290 events.

During the run the current integrator recorded a total flux of 2.17×10^5 microcoulombs of charge and the gamma ray flux through the chamber as measured by the scintillation counter was 4.7×10^6 gammas per cm^2.

The total number of neon atoms in the chamber as calculated from the size of the sensitive volume ($15.2 \times 7.6 \times 7.6$ $cm.^3$) and the pressure (473.5 cm. of mercury) was 1.5×10^{23} atoms.

The cross section from the measured gamma ray flux follows immediately from $\sigma = \frac{Y}{nN}$ and is 4.0×10^{-28} $cm.^2$.

The gamma ray flux from the integrated current was based on the thick target yield figures of Fowler and Lauritsen[49] of 1.90×10^{-8} gammas per proton from the resonance and yield (including the resonance yield) of 2.6×10^{-8} gammas per proton at 850 Kev. for a thick lithium target. The thick target yield for the 650 Kev. bombarding energy used was estimated to be 2.4×10^{-8} gammas per proton. The ratio of 17.6 to 14.8 Mev. gamma rays calculated from the figures of Walker and McDaniel[36] (1.6/1) was used to give a yield of 1.5×10^{-8} gammas per proton of 17.6 Mev. radiation and 0.9×10^{-8} gammas per proton of 14.8 Mev. radiation. The distance of the sensitive volume (mean distance)* was estimated to be 12 cm. Using these figures the cross section was found to be $4.8 \times 10^{-28} cm.^2$, a value in fair agreement with that obtained from the gamma flux measured in the direct way.

---

* Calculated from:- $\frac{V}{r^2} = \int^{\gamma} \frac{dv}{r^2}$

VI. DISCUSSION OF RESULTS

The low cross section for the photo-alpha reaction in Ne^{20} to the ground state of O^{16} and the relatively much larger cross sections to the excited states may be due to the operation of selection rules leading to a decreased probability of a reaction proceeding to the ground state. The relatively larger σ at 14.8 than 17.6 Mev. may perhaps be an indication that the photodisintegration process is sharply energy dependent, the wide gamma-ray energy spread at 14.8 Mev. encompassing regions of large σ whereas the sharp 17.6 Mev. does not. It is difficult to account for the relatively large ratio on the basis of a slow, smooth change in σ for probability of disintegration with hv. If so, this would indicate that the whole nucleus is excited by the interaction of the photon.

By using the non-resonant portion of the cross section for gamma ray production in the $Li^7(p,\gamma)Be^8$ reaction, an experiment is feasible in which the energy of the gamma rays used for the irradiation of the neon is varied. If there is a definite dependence of the cross section for the (γ,α) reaction on energy, further information may be obtained for establishing the mechanism of the interaction between a gamma ray and a nucleus.

PART III

THE DISINTEGRATION OF NEON BY FAST NEUTRONS

I. INTRODUCTION

The study of nuclear energy levels may be carried out by particle excitation as well as by excitation by radiation as was discussed in Part II. In general, low-lying levels of a compound nucleus can not be excited by particles due to the binding energy of the order of 8 Mev. associated with a nucleon. Levels close to the binding energy require slow bombarding particles and if the particles are charged, such as protons, difficulties are experienced in overcoming the Coulomb barrier. Uncharged particles (neutrons) do not experience this difficulty and much useful work has been done using them.

A compound nucleus with an excitation of 8 Mev. or more is most likely to decay by remission of a neutron due to the Coulomb barrier for charged particles. Light nuclei may decay by alpha emission, however, as the number of particles is low and the excitation per particle is therefore high. In this way, fast neutron

disintegrations have been investigated for nitrogen $N^{14}(n,\alpha)B^{11}$[50] and boron $B^{10}(n,\alpha)Li^{7}$[51].

The reaction $Ne^{20}(n,\alpha)O^{17}$ has been investigated by several workers[52,53,54,55]. It is of interest because both the Ne^{21} compound nucleus and the O^{17} residual nucleus are of the $4n+1$ type where an extra neutron has been added to the 4 alpha-particle model of O^{16} and to the 5 alpha-particle model of Ne^{20}, both of which were discussed in Part II. The reaction was established in cloud chambers [56,57] using "natural" neutron sources.

The work of Johnson[54] and of Sikkema[53] is the best to date on the energy levels of Ne^{21} for neutron energies up to 3 Mev. They found transitions to the ground state of O^{17} from several levels in the Ne^{21} compound nucleus. A further investigation of the same reaction was carried out by Flack[55] who obtained resonances corresponding to 15 levels in Ne^{21} from 10 Mev. to 12 Mev. excitation and alpha particle transitions to the .87 excited state of O^{17} as well as to the ground state. The neutrons were produced by the well known $D(d,n)He^{3}$ reaction[58]. Neutrons of 5 Mev. energy are produced in this reaction with a deuteron bombarding energy of 2 Mev. and the neutrons into a small, solid angle in the forward direction are closely monoenergetic.

It was felt that the use of neutrons of still higher energy would enable higher levels of Ne^{21} to be measured from reaction resonances and would also give evidence for higher energy levels in the O^{17} nucleus. Since tritium targets became available to the laboratory from the N.R.C. pile at Chalk River, the high

energy neutron source $H^3(d,n)He^4$ could be used for producing the neutron flux. This reaction has a Q of 17.6 Mev. giving a neutron energy of 14.1 Mev. at zero bombarding energy.

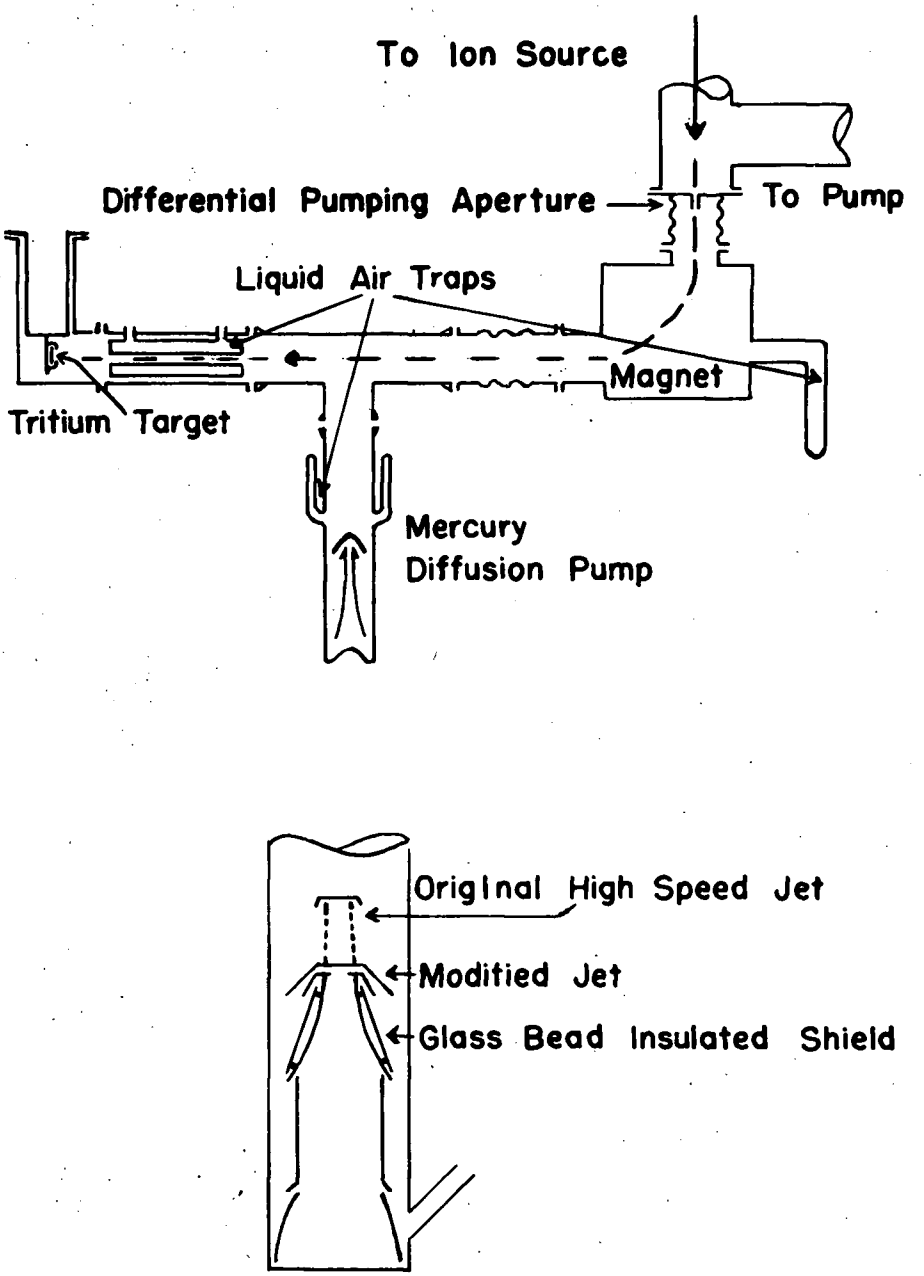

Fig. XXVI Experimental Arrangement for Neutron Bombardment of Neon

II. EXPERIMENTAL TECHNIQUE

The neon gas was contained in the same gridded ionization chamber as discussed in Part II.

The tritium target used in the experiment was absorbed on a tantalum layer melted on to a tungsten backing. The exact thickness of the target was not known, but was perhaps as much as one hundred kilovolts. The plate carrying the target was mounted on a copper back which was water-cooled (Figure XXVI).

Considerable modifications were made to the vacuum system of the 50 kv accelerating set built by Kirkaldy[59] to prevent cracked oil products and backstreaming oil vapours from the pumps from getting into the system. The baffle system for the main diffusion pump was modified, a second diffusion pump (Hg vapour) was added and with suitable cold traps throughout the system, this effect was reduced to a large extent; 2000 microampere hours of bombardment resulted in a decrease in neutron flux of a factor of 3 and only a very slight darkening of the surface of the tritium target. At the end of this time the target contained a large amount of absorbed D from the beam, which caused the production of (D-D) neutrons.

The neutron flux was monitored by a long boron counter in paraffin* of the type discussed by Hanson and McKibben[60], with an efficiency of 1/250 per neutron impinging on the sensitive area.

---

* Mr Heiberg constructed the neutron Monitor.

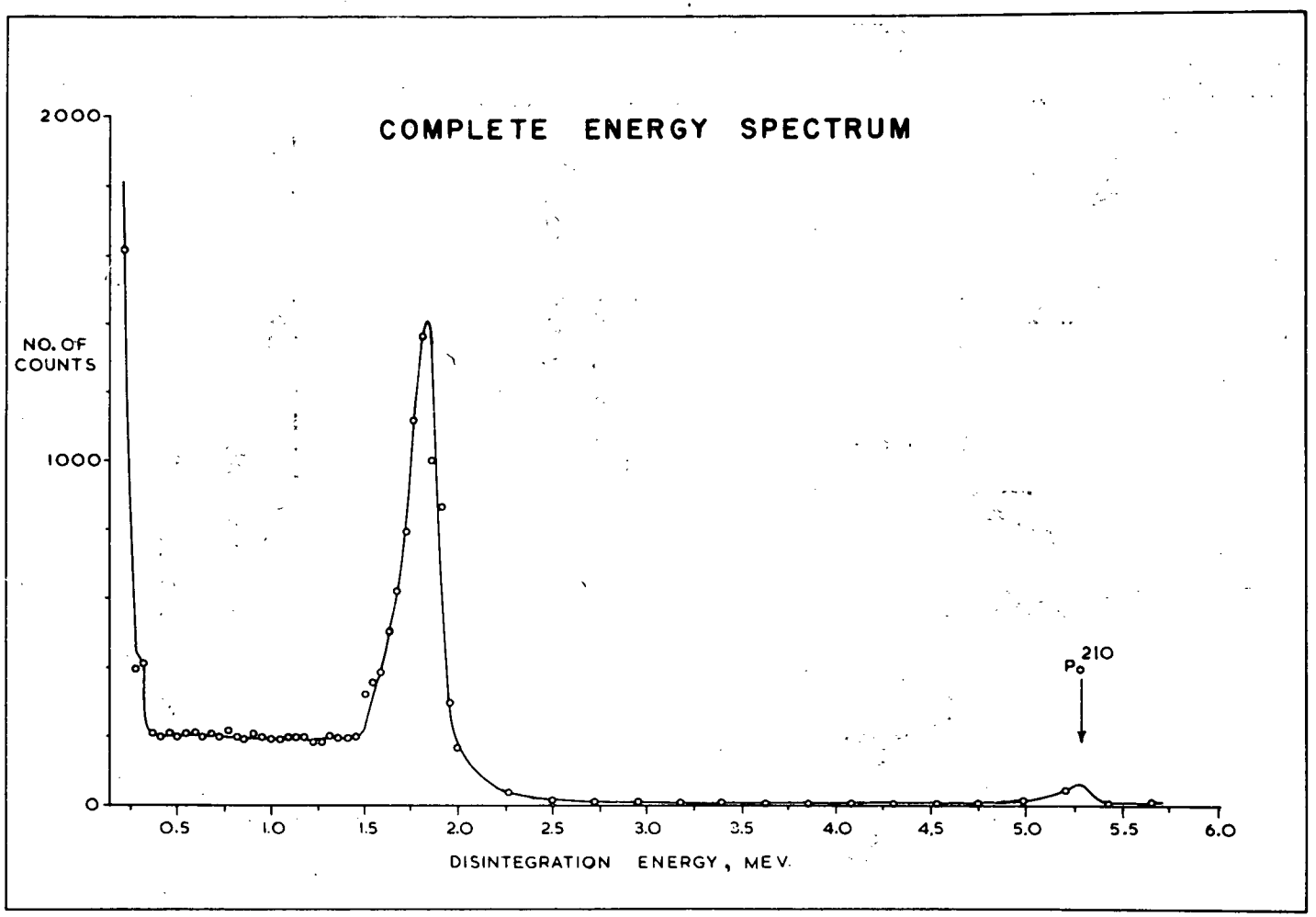

Fig. XXVII Pulse Spectrum of (D-D) Neutrons on Neon

III. EXPERIMENTAL PROCEDURE

The neon gas contained in the ionization chamber was bombarded with neutrons from the d-on d reaction using a heavy-ice target. The spectrum of pulses so obtained is displayed in Figure XXVII. The peak in the distribution is due to the reaction $Ne^{20}(n,\alpha)O^{17}$ ground state which has a Q of -.70 Mev. as measured by both Phillips[38] and Flack[39].

The tritium target was placed in position and bombarded with a flux of about 100 microamps of resolved protons at 50 kilovolts bombarding energy. The neutron flux as measured by the monitor was 2×10^7 neutrons per second at the target. The kick-sorter was set up to record the pulse height spectrum in 75 kilovolt steps beginning at 1 Mev. When sufficient counts had been obtained, the unit was set up to cover the next energy range in the same channel widths and the procedure was repeated until the whole spectrum had been covered to 14 Mev. The distribution obtained in this way is plotted in three sections which are given in Figures XXVIII, XXIX and XXX. The region below 4 Mev. is not plotted as the distribution was a monotonically-rising function in this region and had no interesting features.

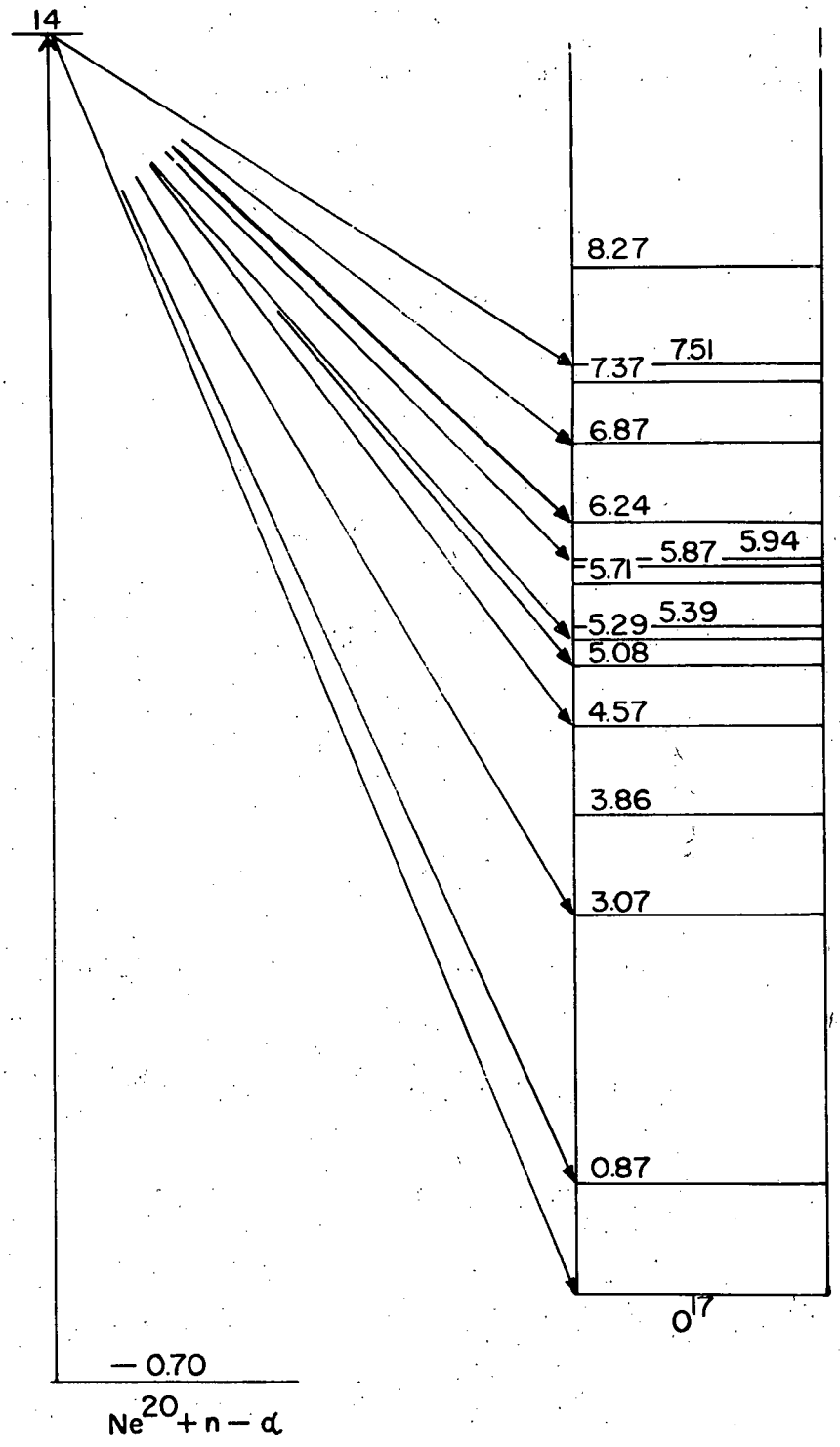

Fig. XXXI Observed Alpha Groups to Levels in O^{17}

IV. RESULTS

The pulse height distribution shows a large number of peaks superimposed on a large background at energies below 7.8 Mev., which is the maximum range of protons in the chamber as outlined in Section II. The background may be attributed to (n, p) processes in the walls and in the gas itself.

The peaks correspond to energy release in the chamber of 13.3, 12.3, 10.25, 8.70, 8.20, 7.85, 7.30, 6.95, 6.50, 5.93 and 5.72 Mev. From the energy-level diagram as given by Ajzenberg and Lauritsen[48], it is seen that these values are in very good agreement with the energy levels of O^{17} at 0, .87, 3.06, 4.56, 5.08, 5.31, 5.94, 6.24, 6.87, 7.37, and 7.51 Mev. The transitions involved in the reaction are shown on the diagram in Figure XXXI.

Since (n,p) processes in neon arise from the reaction $Ne^{20}(n,p)F^{20}$ and this reaction has a Q of -6.25 Mev.[48], only the lowest three peaks in the pulse height distribution curve may be said to be in doubt due to (n,p) processes to levels in F^{20}.

The agreement of the energy values is so good, however, that it is doubtful that the peaks do represent (n,p) processes. Additional verification of these levels in O^{17} are given by the measurements. In particular, the level at 8.07 Mev., which was doubtful in the summary of Ajzenberg and Lauritsen, has received additional support.

APPENDIX I

Rayliegh Scattering

Coherent scattering of gamma radiation from electrons which are bound to atoms is known as Rayliegh scattering. This is distinguished from nuclear scattering of gamma radiation which has been called Thomson scattering.

Coherent scattering from the bound electrons is essentially an interference effect. The amplitudes of the gamma ray scattered by the electrons, with their various phases, must be summed over all the electrons in an atom. The electron distribution must therefore be known to some degree of approximation. The best approximation is given by the Hartree model, but for large Z the Fermi-Thomas gas cloud model is equally valid.

The method of evaluating the cross section is given in Compton and Allison* and has been worked in detail by Franz[10], who has evaluated the cross section for hard radiation.

The Fermi-Thomas distribution for the electrons may be expressed by: $g(a)da = 2.13Z^{1/3}\left(\frac{a}{\alpha}\right)^{1/2}\left[\phi\left(\frac{a}{\alpha}\right)\right]^{3/2}da$

where Z is the atomic number and α is a radius characteristic of the atomic number Z, defined by $.47\ Z^{-1/3}$ angstroms. The electronic structure factor, f, is given by the equation

$$\int_0^\infty g(a)\frac{\sin k(a)}{ka}da \qquad \text{where} \quad k = \frac{4\pi}{\lambda}\sin\theta/2$$

The angle θ is the direction of scattering.

---

* Compton and Allison - X rays in Theory & Experiment Van Nostrand 1935

The scattering factor is then Zf^2. Debye has evaluated this function for large Z and has plotted the scattering amplitude as a function of the scattering angle[11]. This function is reproduced in Figure VIII, where the differential scattering amplitude is plotted against u where $u = \frac{4\pi}{\lambda} \alpha \sin \theta/2$. For .51 Mev. radiation u becomes $2.43 \times 10^2 Z^{-1/3} \sin \theta/2$.

APPENDIX II

Direct Flux Measurement by NaI(Tℓ) Crystal

The intrinsic efficiency for pair production and Compton effect of the NaI crystal can be calculated from the theoretical cross sections for both of these effects for the 17.6 and the 14.8 Mev. gamma rays of the $Li(p,\gamma)Be^8$ reaction. The wall effect in the crystal will reduce the energy dissipated by the secondary electrons in some cases, and further, some secondaries will produce bremstrahlung which may escape from the crystal and so reduce the energy released therein.

The fraction of the maximum efficiency which is utilized by biasing the counter at a level corresponding to an energy dissipation of 10.5 Mev. in the crystal may be deduced from the shape of the pulse spectrum obtained (Figure XXI). This approximation is helped by comparison with the spectrum obtained from the single gamma ray in the $p + d \rightarrow He^3 + \gamma$ reaction[45]. Since 50% of the spectrum lies above the 10.5 Mev. energy level, the fractional efficiency is most certainly accurate within 20% limits.

The NaI crystal was cylindrical in shape of a diameter of 4.46 cm. and a length of 5.08 cm. The cross sections for absorption of the 17.6 and 14.8 Mev. gamma radiation are 8.77 and 7.92 x 10^{-24} cm.^{2} per molecule of NaI, neglecting the effect of the (Tℓ).

The intrinsic efficiency of the crystal as calculated from these values is .557 for the 17.6 Mev. gamma rays and .538 for the 14.8 Mev. radiation. The fraction of this maximum efficiency which is utilized is 0.70 ± .15 and 0.59 ± .12 respectively.

The absorption of the chamber walls was taken into consideration by measuring its magnitude by inserting the chamber between the target and the gamma ray monitor. The fraction absorbed in this way was 0.40 ± 0.05. The gamma ray flux was monitored during the course of the experiment with the chamber in this position.

By defining:

w = solid angle subtended by the monitor

ε = intrinsic efficiency

f = fraction of maximum efficiency utilized

b = fraction absorbed by ionization chamber. This fraction is assumed equal for 14.8 and 17.6 Mev. gammas.

No = number of disintegrations in target giving rise to gamma rays

Nc = number of counts in counter due to gamma rays without chamber absorption

Np = number of counts in counter with chamber absorption

and if these same quantities for 14.8 and 17.6 Mev. gamma rays are defined by superscripts 14 and 17, then:

$$N_c = \frac{N_p}{1-b} = w\, N_0^{17}\left(\varepsilon^{17} f^{17} + \frac{N_0^{14}}{N_0^{17}}\,\varepsilon^{14} f^{14}\right)$$

The ratio of $\frac{N_0^{14}}{N_0^{17}}$ may be obtained from the curves of Walker and McDaniel as previously described. Since the flux into the ionization chamber is only reduced by b/2, (there is only one wall between the volume of the chamber and the target) the flux/cm^2 in the chamber is given by: $N^{17} = \frac{1}{4\pi d^2}\left(1 - b/2\right) N_0^{17}$

d = mean distance of the sensitive volume of the chamber.

BIBLIOGRAPHY

1.	Heitler,	The Quantum Theory of Radiation Oxford,	P231,	(1944)
2.	De Benedetti, Cowan, Kenneker and Primakoff,	Phys. Rev.,	77, 205	(1950)
3.	Argyle and Warren,	Can.J.Phys.,	29:32	(1951)
4.	Griffiths and Warren,	Can.J.Phys.,	29:325	(1951)
5.	Maier - Leibnitz, H.,	Zeits. für Nat.,	11 665	(1951)
6.	Bell, Graham and Petch,	Can.J.Phys.,	30:35	(1950)
7.	Silver, Miss L.M.,	Can.J.Phys.,	29:59	(1951)
8.	Moon,	Proc. Phys.Soc. London,	A63, 1189	(1950)
9.	Storruste,	"	A63, 1197	(1950)
10.	Franz,	Zeits.für Phys.,	98, 314	(1935)
11.	Debye,	"	317, 98	(1935)
12.	Deutsch,	Phys. Rev.,	82, 455	(1951)
13.	Bell,	Private Communication.		
14.	Chadwick & Goldhaber,	Nature,	137, 1234	(1934)
15.	Wheeler,	Phys. Rev.,	52, 1083	(1937)
16.	Barnes, French & Devons,	Nature,	166, 145	(1950)
17.	Goldhaber & Teller,	Phys. Rev.,	74, 1045	(1948)
18.	Levinger and Bethe,	Phys. Rev.,	78, 115	(1950)
19.	Courant,	"	82, 703	(1951)
20.	Baldwin and Koch,	"	67, 1	(1945)
21.	McElhinney, Hanson, Becker, Duffield & Diven,	"	75, 542	(1949)

22. Johns, Katz, Douglas & Haslam, Phys. Rev., 80:1062 (1950)

23. Halpern & Mann, " 83, 370 (1951)

24. Preston, " 80, 307 (1950)

25. Goward, Telgedi & Wilkins, Proc. Roy. Soc., A63, 402 (1950)

26. Wäffler & Younis, Helv. Phys. Acta., 22, 614 (1949)

27. Woods, Unpublished thesis, U.B.C.

28. Wilkinson, Ionization Chamber & Counters, (1949)
Cambridge University Press.

29. Frisch, British A.E.R.E. Report BR-49.

30. Bunemann, Cranshaw & Harvey, Can. J. Research, A27, 191 (1949)

31. Gray, Proc. Camb. Phil. Soc., 40, 95 (1944)

32. Jesse, Forstat and Sadauskis, Phys. Rev., 77, 782 (1950)

33. Cranshaw and Harvey, Can. J. Research, A26 743 (1946)

34. Hanna, Phys. Rev., 80 530 (1950)

35. Tangen, Det. Kgl. Norske vid. Sels. Skrifter, NRI, (1946)

36. Walker and McDaniel, Phys. Rev., 74, 315 (1948)

37. Jentsche and Prankl, Phys. Zeits., 41, 524 (1939)

38. Phillips, M.A. Thesis U.B.C., (1952)

39. Flack, Report on Fast Neutrons in Neon, U.B.C. (1952)

40. Elmore and Sands, Electronics Experimental Techniques- McGraw Hill, 167, (1949)

41. Westcott and Hanna, Rev. Sci. Inst., 20, 181 (1949)

42. Bowers, Private Communication

43. Swank and Moenich, R.S.I., 23 502 (1952)

44. Azuma, M.A. Thesis, U.B.C. (1953)

45. Griffiths, PhD. Thesis, U.B.C. (1953)

46. Klemperer, Proc. Camb. Phil. Soc., 30, 347 (1934)

47. Beringer & Montgomery, Phys. Rev., 61, 222 (1942)

48. Ajzenberg and Lauritsen, Rev. Mod. Phys., 24, 321 (1952)

49. Fowler and Lauritsen, Phys. Rev. 76, 314 (1949)

50. Johnson and Barschall, Phys. Rev. 80, 818 (1950)

51. Adair, Rev. Mod. Phys., 22, 249 (1950)

52. Graves and Coon, Phys. Rev., 70, 101 (1946)

53. Sikkema, Nature, 165, 1016 (1950)

54. Johnson, Bockelman & Barschall, Phys. Rev., 82, 117 (1951)

55. Flack, Report on Disintegration of Neon by Fast Neutrons, unpublished, U.B.C., (1952)

56. Harkins, Gans & Newson, Phys. Rev., 47, 52 (1935)

57. Zagor and Valente, Phys. Rev., 67, 133 (1945)

58. Oliphant, Harteck and Rutherford, Proc. Roy. Soc., A144, 692 (1934)

59. Kirkaldy, M.A. Thesis, U.B.C. (1951)

60. Hanson & McKibben, Phys. Rev., 72, 673 (1947)

61. Mattauch & Flammersfeld, Isotopic Report; Tubingen, (1949)

62. Sample, Unpublished report on Particle Detector U.B.C., (1953)